CONDUCTION MECHANISMS FOR ELECTRONIC DEVICES

DAVID REDFIELD AND ISAAC BALBERG

RCA LABORATORIES
PRINCETON, NJ 08540

FINAL REPORT

JUNE 1972

CONTRACT N00014-71-C-0371

U. S. DEPARTMENT OF THE NAVY
OFFICE OF NAVAL RESEARCH
WASHINGTON, DC 20390

UNCLASSIFIED

Security Classification

DOCUMENT CONTROL DATA - R & D

(Security classification of title, body of abstract and indexing annotation must be entered when the overall report is classified)

1. ORIGINATING ACTIVITY (Corporate author) RCA Laboratories Princeton, N.J. 08540	2a. REPORT SECURITY CLASSIFICATION Unclassified 2b. GROUP N/A

3. REPORT TITLE

CONDUCTION MECHANISMS FOR ELECTRONIC DEVICES

4. DESCRIPTIVE NOTES (Type of report and inclusive dates)

Final Report 3 May 1971 to 2 May 1972

5. AUTHOR(S) (First name, middle initial, last name)

David Redfield
Isaac Balberg

6. REPORT DATE	7a. TOTAL NO. OF PAGES	7b. NO. OF REFS
June 1972	83	144

8a. CONTRACT OR GRANT NO.	8a. ORIGINATOR'S REPORT NUMBER(S)
N00014-71-C-0371	PRRL-72-CR-26
b. PROJECT NO.	
c.	9b. OTHER REPORT NO(S) (Any other numbers that may be assigned this report)
d.	

10. DISTRIBUTION STATEMENT

11. SUPPLEMENTARY NOTES	12. SPONSORING MILITARY ACTIVITY
	U. S. Naval Research Laboratory Washington, D.C. 20390

13. ABSTRACT

PART I: Controllable electronic energy band tails have been prepared in heavily doped, closely compensated GaAs. Their properties are found to correspond in many ways with the reported properties of amorphous semiconductors. The control now over the occupation of the band tail states permits observation of the energy dependence of various transport properties, (temperature dependence of the d.c. conductivity, frequency dependence of the a.c. conductivity and current-voltage relations). These measurements display evidence contrary to the notion of a sharp mobility edge. Our theoretical work on statistical influences on these properties shows that sharp mobility edges are less probable than generally believed, for amorphous semiconductors as well as these materials. The electric field dependence of the conductivity in several samples is nearly exponential over several decades; possible applications are discussed.

PART II: We have studied the electronic properties of Fe_3O_4 and VO_2. These materials are the only ones that show satisfactory switching effects due to the insulator to metal transition. The possibility of switching due to dissociation of polarons was examined theoretically as well as experimentally using oxygen-reduced TiO_2. We have found that the band structure of Fe_3O_4 can be discussed in terms of crystal field splitting and correlation effects. Experimental evidence indicates that the transition is of the Mott-Wigner type. In the study of VO_2 we have demonstrated the versatility of VO_2 films for new effects and applications and were able to conclude that the V-V separation along the c-axis is the most important parameter in determining the transition temperature. The theoretical and experimental study on the possibility of "polaron switching" led to the conclusion that the mechanism proposed by Hed and Freud is unfounded theoretically and is not feasible experimentally.

DD FORM 1 NOV 1473

UNCLASSIFIED

Security Classification

14 KEY WORDS	LINK A		LINK B		LINK C	
	ROLE	WT	ROLE	WT	ROLE	WT
Disordered Semiconductors						
Energy Band Tails						
Electronic Transport Properties						
Transition Metal Oxides						
Polaron Switching						
Magnetite Properties						
Rutile Properties						

14

FOREWORD

This Final Report was prepared by RCA Laboratories, Princeton, N.J., under Contract N00014-71-C-0371. It describes work done during the period 3 May 1971 to 2 May 1972 in the Physical Electronics Laboratory, G. D. Cody, Director. The Project Supervisor was R. Cohen and the Project Scientist was D. Redfield. A significant part of the research and Part 2 of this report were done by I. Balberg.

The report itself is organized in two parts, both parts including references and appendices. Each of the four appendices either was published or is to be published shortly.

ABSTRACT

PART 1: Controllable electronic energy band tails have been prepared in heavily doped, closely compensated GaAs. Their properties are found to correspond in many ways with the reported properties of amorphous semiconductors. The control now possible over the occupation of the band tail states permits observation of the energy dependence of various transport properties (temperature dependence of the d.c. conductivity, frequency dependence of the a.c. conductivity and current-voltage relations). These measurements display evidence contrary to the notion of a sharp mobility edge. Our theoretical work on statistical influences on these properties shows that sharp mobility edges are less probable than generally believed, for amorphous semiconductors as well as these materials. The electric field dependence of the conductivity in several samples is nearly exponential over several decades; possible applications are discussed.

PART 2: We have studied the electronic properties of Fe_3O_4 and VO_2. These materials are the only ones that show satisfactory switching effects due to the insulator to metal transition. The possibility of switching due to dissociation of polarons was examined theoretically as well as experimentally using oxygen-reduced TiO_2.

We have found that the band structure of Fe_3O_4 can be discussed in terms of crystal field splitting and correlation effects. Experimental evidence indicates that the transition is of the Mott-Wigner type. In the study of VO_2 we have demonstrated the versatility of VO_2 films for new effects and applications and were able to conclude that the V-V separation along the c-axis is the most important parameter in determining the transition temperature.

The theoretical and experimental study on the possibility of "polaron switching" led to the conclusion that the mechanism proposed by Hed and Freud is unfounded theoretically and is not feasible experimentally.

TABLE OF CONTENTS

TABLE OF CONTENTS (Continued)

LIST OF ILLUSTRATIONS

LIST OF ILLUSTRATIONS (Cont'd.)

LIST OF ILLUSTRATIONS (Cont'd.)

PART 1

DISORDERED SEMICONDUCTORS

by

David Redfield

PART 1 - DISORDERED SEMICONDUCTORS

I. INTRODUCTION

Widespread interest and activity in amorphous semiconductors have recently been generated by the apparent promise of new device potentialities as well as the intrinsic interest in a new class of materials. A major development in this field, however, has been the demonstration that most of the devices made from amorphous semiconductors do not operate by electronic processes as initially thought[1] but rather by thermally induced phase changes. Nevertheless, there is no known reason that precludes the existence of *electronically* active devices based on their electronic properties[2] and, if available, they could have important advantages such as higher speed, greater reproducibility, and better controllability. Thus, there are good reasons to seek new approaches to the understanding and control over the electronic behavior of amorphous semiconductors.

The present program is motivated in part by those considerations and in part by the recognition that amorphous semiconductors are a subgroup of the broader class of materials, disordered semiconductors, which also include heavily doped crystalline semiconductors which are in wide use in numerous types of devices. These latter materials also have major advantages over *all* amorphous semiconductors in that they can be controllably prepared, their properties are much better understood, and they are known to be electronic in their operation. Therefore, it would be highly desirable to utilize heavily doped crystalline semiconductors in the study of disordered materials provided that their similarities to amorphous semiconductors could be demonstrated.

That has been the goal of this program. The underlying justification for using heavily doped crystalline materials for this purpose is that they are known to have electronic energy band tails which are the key factor in the electronic properties of *all* disordered semiconductors (including amorphous)[2]. Furthermore, with this goal in mind we have developed a process for preparing samples in such a way as to maximize the similarity to amorphous semiconductors and simultaneously allow control over the population of the electronic states in the band tail. This control is of paramount importance in seeking the energy dependence of the properties of the band tail states.

Because they are unique and of central importance, a brief description of the sample preparation techniques and their rationale is in order[3]. As starting material we use high-quality, single crystal GaAs doped with 2-3 x 10^{18} donors/cm^3. This type of material is known to possess band tails [4, 5], but they are not prominent because the strongly

degenerate nature of the material causes the filling of many of the more numerous, band-like states at higher energy as well as the tail states. Wafers of the starting material are made by cutting and lapping to thicknesses of about 1/2 mm. Each wafer is then subjected to copper diffusion in a sealed, evacuated quartz ampoule at 700°-800°C for 2-3 days. The copper produces (deep) acceptor states[6] whose concentration can be made very nearly equal to the donor concentration. This near-compensation causes several important changes that are favorable for the desired simulation of amorphous materials. First, the population of electrons in the conduction band is greatly reduced so those remaining will be only in states of the conduction band tail (the lowest available energy levels). Second, the nearly compensated sample then contains ions of negative as well as positive charge so the potential fluctuations are increased. Since these fluctuations are responsible for the existence of band tail states, the tails are enhanced, making the samples resemble the amorphous semiconductors. Finally, the reduction in concentration of "free" electrons reduces greatly the screening of the potentials, resulting in a further increase in the energy range of the band tails. The samples can then be represented schematically by Figure 1-1 in which the density of states as a function of energy appears

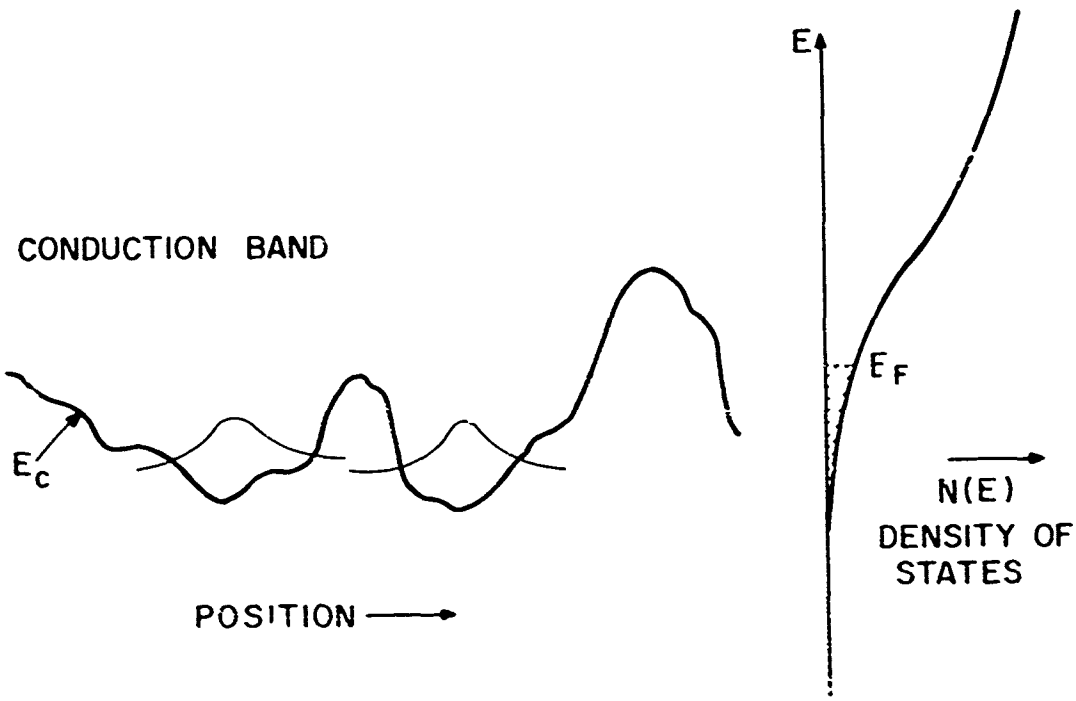

Figure 1-1. A conduction band tail in two representations. The right side shows the spatially averaged density of states, occupied up to E_F. On the left is the corresponding potential as a function of position showing schematically two quasi-localized states of the tail in light lines.

on the right with the shaded region occupied. The potential as a function of position is indicated in exaggerated fashion on the left. The wave functions for two occupied states of the tail are drawn in light lines at regions of low electronic potential. The central feature of band tail properties is the tendency of the lower energy states to be localized in space by the fluctuations of the potential. Indeed, the concept of a "mobility edge" is simply a way of describing an abrupt step in that energy dependence of the localization[2].

In our samples - in contrast to the amorphous semiconductors - the extent and even the shape of band tail density of states are known to some extent, and the occupation level of the electrons in the tail states can be controlled by our compensation process. The final steps of this process are precisely timed irradiation with 1-MeV electrons in our Van de Graaff generator. Such irradiation is known to produce (deep) acceptors[7] which increase the compensation in a precisely controllable manner. Thus, the same sample can be measured, further compensated, and remeasured to determine the effect of lowering the Fermi level in the band tail. In this way we achieve direct observation of the energy dependence of the various properties and thereby a picture of the way in which localization of the states influences those properties.

II. SAMPLE PREPARATION

A substantial effort has been devoted to developing, refining and analyzing the preparative techniques which are so crucial to this program. The first step is choice of the initial donor dopant. The availability of high-quality Si-doped GaAs made it the original choice. Subsequent experiments have used Se or Te doping which have been found to be generally less desirable than the Si, possibly because of precipitation of the dopants at the high concentrations used here. It is well known that Si has a higher solubility in GaAs than these other common donors, and so it is now used regularly.

Another series of preparations was undertaken to try to incorporate both donors and acceptors into the grown crystal, thus bypassing the need for copper diffusion. For this purpose liquid phase epitaxial layers were grown on GaAs substrates. This effort was promising in some respects but always resulted in unacceptably high inhomogeneity through the layer thickness. Another approach to this objective utilized slices of commercially bought GaAs which was supposedly double-doped in roughly the desired way. Evaluation of these wafers showed them to be much more inhomogeneous than any other material and therefore not suitable to our needs.

The next aspect of the preparation process investigated is the copper diffusion. Several methods were used to improve the reproducibility of this step. Controlled evaporation of copper onto the wafer surface did not seem to improve the results compared with the simpler flash evaporation of copper in the ampoule. In either case, the subsequent heat treatment had to be carried on for at least two days using temperatures generally near 700°C. It is also easy for excess copper or diffusion time to cause type conversion, thus rendering a wafer useless for our purposes. Some limited experiments were carried on to determine the effect of excess As during diffusion, but the results were inconclusive.

One of the major problems inherent in such materials is inhomogeniety of the dopants. This is exacerbated by the very close compensation we require since that serves to amplify existing nonuniformities. Such inhomogenieties may arise from the original donor distribution, the effects of copper diffusion or the irradiation by 1-MeV electrons. The first is probably already minimized by the use of high-quality starting material and cannot be reduced further. The second may be influenced by the one-dimensional character of the copper diffusion, causing the center layer of a wafer to be less compensated. The high-energy electron beam can also produce a compensation gradient through the thickness of the sample. We have studied the latter two effects by detailed measurements of the profiles of several wafers treated in different ways. The results indicate that the two-day diffusion time is adequate to eliminate layer-like variations

in copper concentration. However, it has been found that 1-MeV electrons cannot produce a satisfactorily uniform defect distribution in GaAs thicker than ∿ 10 mils. This presents a rigid upper bound on sample thickness although we can nearly double it by irradiation on both sides of the wafer.

The final aspect of our preparative work concerns the nature of electrical contacts to these samples. It is notoriously difficult to make good ohmic contacts to high-resistance materials, and we have found these to be no exceptions. At low temperatures some of these materials possess very high resistivities and contact problems were severe. We have found, however, two measures that have nearly eliminated those difficulties. First is the use of In-Sn alloys for contact materials. These are alloyed into the samples in conventional ways after copper diffusion but before electron beam irradiation. This is an important sequence because the sample resistivities are still low before irradiation and the formation of good contacts is easier. (In addition, it is not possible to alloy in contacts after electron beam irradiation because the heating process anneals out the radiation-induced acceptors.) The second advance is the use of thick Ta masks to shield the contact regions on 6-arm samples during the irradiation. This maintains each contact area in a low-resistivity state, with the transition to high-resistivity, irradiated material occurring in the GaAs away from the contact. These steps have been very effective on samples having side-arms but not always successful on wafer-shaped samples with contacts covering essentially their entire faces so that masks cannot be used.

III. MEASUREMENTS

Several types of measurements have been made to determine the electronic properties of the band tail states and to compare them with those of amorphous semiconductors. They will be presented separately but they have been used collectively both to characterize the tail states and to evaluate the various preparation techniques.

After the preliminary Hall effect and conductivity measurements[3] it was decided that there were too many uncertainties in the interpretation of the Hall effect in band tails to justify its immediate continuation. Therefore, the simplest possible conductivity measurements have been stressed in this work.

A. D.C. CONDUCTIVITY AS A FUNCTION OF TEMPERATURE

This type of measurement, made with 4-probe samples having sidearms with masked contacts, is the first and most extensive one. Temperatures can be accurately controlled between 2 K and 300 K; samples were cooled in the dark and measured with very low currents flowing through them. All normal precautions showed that there were no heating effects due to the measuring current, no contact effects or thermal gradient effects in the results. Reproducibility of the properties was not a problem.

The initial measurements showed that as the compensation was made to approach 1 the temperature dependence of the conductivity became exceedingly strong[3]. We have found a way of confirming the band tail interpretation of that effect by the following experiment which takes advantage of the inhomogeneities that are generally undesirable. Two samples cut from opposite ends of the same wafer (after copper diffusion) were found to have rather different temperature dependences of their conductivities $\sigma(T)$. These are shown in Figure 1-2 as #3 and #4; it is evident that both the magnitude and the curve shape are quite different. After these data were obtained the higher-conductivity sample was irradiated with 1-MeV electrons just long enough to equalize its *room-temperature* conductivity with that of the other sample. Then $\sigma(T)$ was remeasured for the irradiated sample and found to coincide completely down to 4.2 K.

This result is of great importance to the entire program because it offers strong confirmation that the observed properties are indeed attributable to band tails and not to any specific properties of the impurities or defects present in the samples. The changes in $\sigma(T)$ must really be a result of lowering the Fermi level in the tail regardless of how that lowering is brought about.

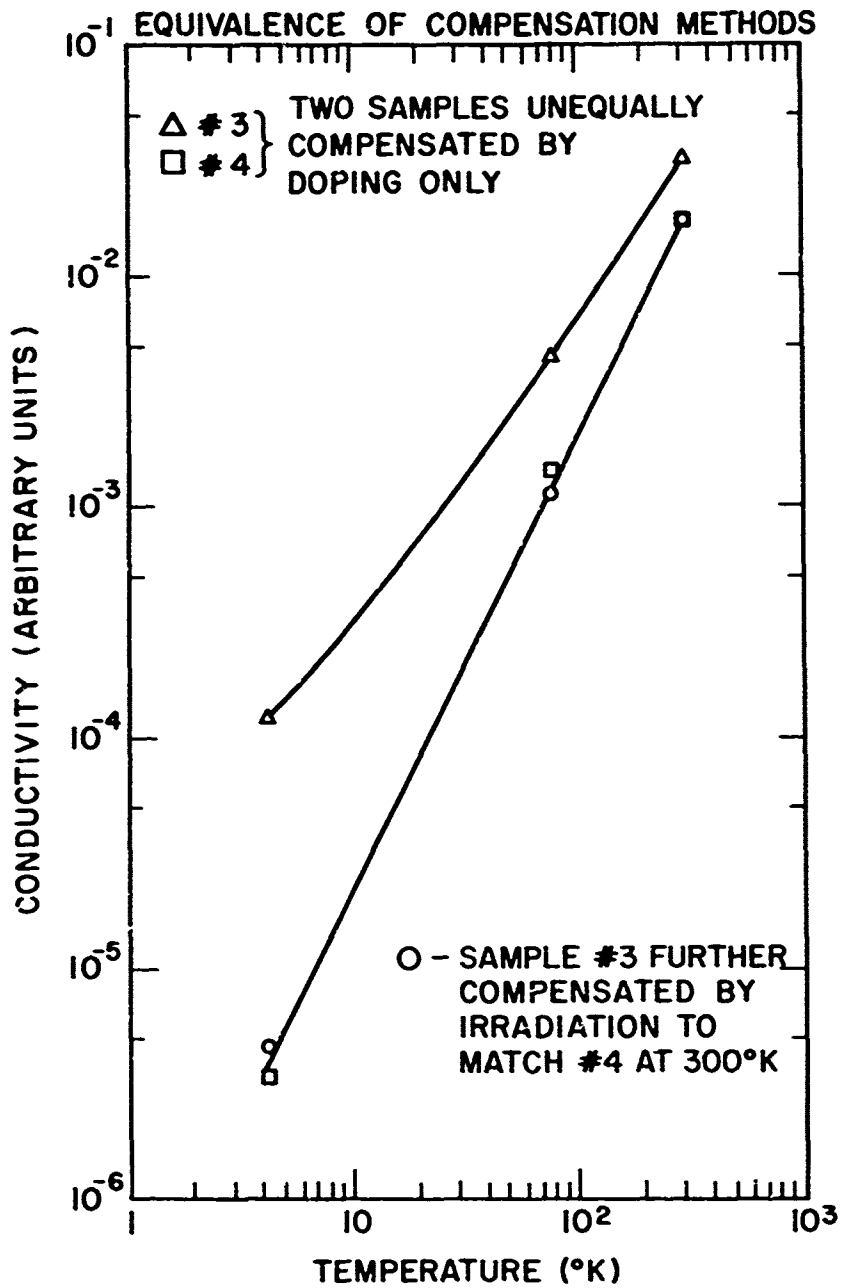

Figure 1-2. Equivalence of behavior of two samples brought to their final compensation level in different ways. Δ and □ denote intial properties of the two samples having been copper-diffused. O denotes the properties of sample Δ after irradiation by 1-MeV electrons so as to match the σ (300 K) of sample □ .

One potential application of these band tails is also apparent in Figure 1-2 - low-temperature thermometry. Two features are particularly noteworthy. First is the strong temperature sensitivity which can be realized over a wide range of temperatures. Second is the ease with which this sensitivity can be controlled by our compensation techniques. To test the usefulness of this device we fabricated a sample so as to exceed somewhat the temperature sensitivity of our commercial Ge resistance thermometer at 4.2 K ($\sim$ 300 Ω/K). Then the temperature sensitivity was measured up to $\sim$ 200 K. It turned out that this device had a higher sensitivity than the *combination* of the Ge and Pt resistance thermometers to above 100 K. It is now clear that thermometers can be easily fabricated this way to have high sensitivities in any desired range up to $\sim$ 200 K.

The dc conductivity, $\sigma(T)$, offers one ready means of comparing the properties of known band tails with the observations in the largely uncertain amorphous semiconductors. To this end we have made detailed measurements of $\sigma(T)$ between 2 K and 300 K and plotted the results in the manner used for those materials. Several theories[8,9] for their behavior predict that $\log \sigma \sim (T_o/T)^{1/4}$, and some reports of such behavior in amorphous Ge and Si have been published[10]. For comparison we have plotted our data as $\log \sigma$ vs. $T^{-1/n}$ with $1 \leq n \leq 5$. The results for three of these are shown in Figure 1-3 for a sample prepared so as to change by six orders of magnitude. This exhibits clearly one of the significant advantages available with these materials because such control of sample properties permits measurements to be made over a temperature range 30 times as great as reported for a Ge and a Si[10]. The three curves of Figure 1-3 all display the same data between 2 K and 300 K; only the abscissa scale is different for each. Clearly, T^{-1} cannot be fit with any straight line; thus, no single activation energy is responsible. Both $T^{-1/2}$ and $T^{-1/4}$ give fairly good fits to straight lines, but with *two* segments. ($T^{-1/3}$ is similar, but $T^{-1/5}$ has a distinctly poorer fit to straight lines.) Thus, we find a similarity to the amorphous semiconductors but with a new observation which might be attributable to the much wider temperature range used here. It should be noted that the same type of behavior was observed in a less closely compensated sample whose conductivity varied by only two decades over the same temperature range. This appears particularly significant because that conductivity is always much higher than the values normally associated with "hopping conduction" for which the $T^{-1/4}$ theory was derived. Thus, this 2-segment "linear" fit offers a challenge to the theories of disordered semiconductors. Further, the ability to fit the data well with $\log \sigma \sim T^{-1/2}$ has opened some interesting new lines of interpretation.

B. FREQUENCY DEPENDENCE OF A.C. CONDUCTIVITY

This type of measurement was important principally because all amorphous semiconductors (as well as many other insulators) exhibit the

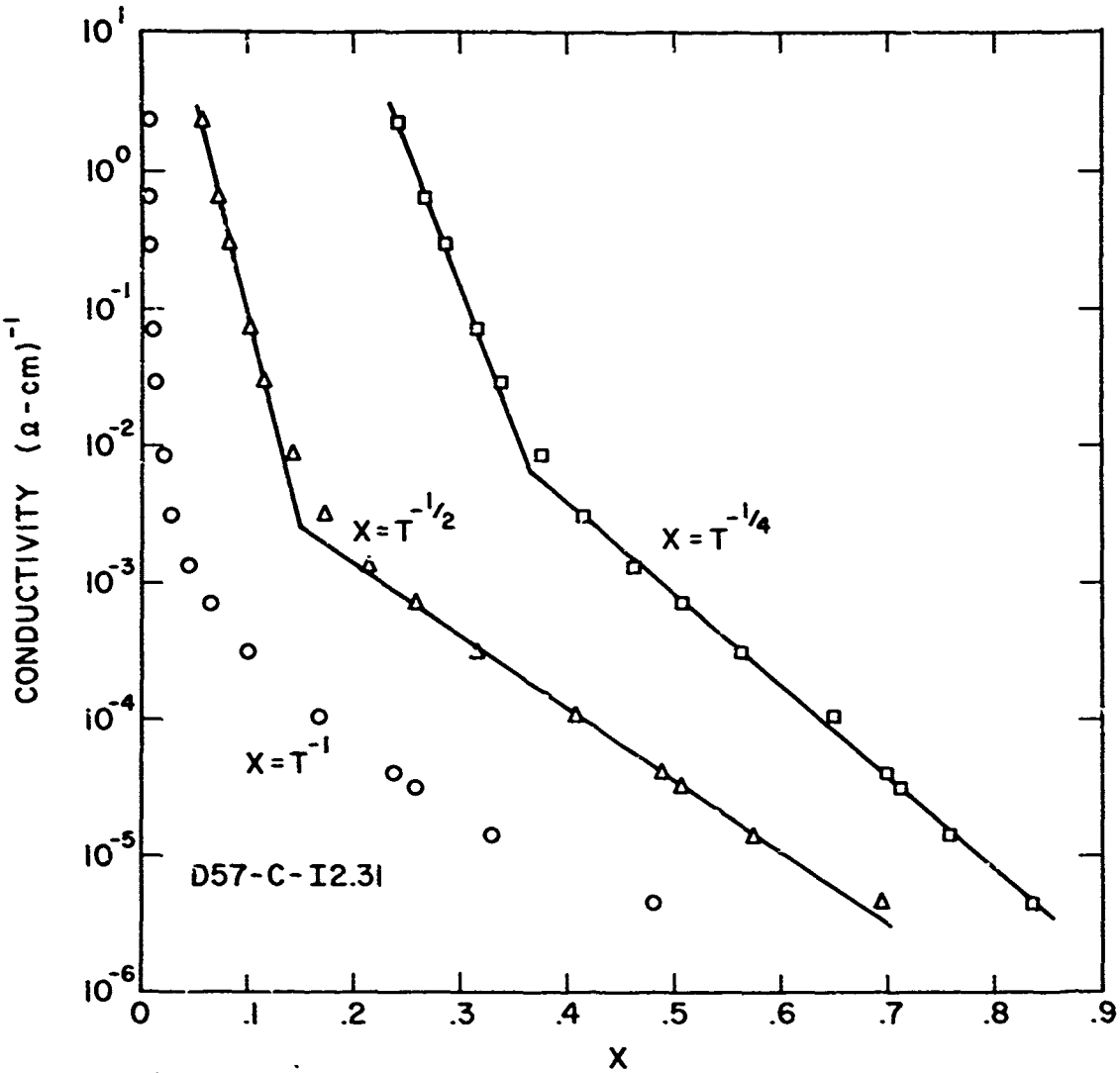

Figure 1-3. Temperature dependence of the conductivity between 2 K and 300 K for a single sample plotted with three different abscissas. This displays the good 2-segment, linear fit of log σ with either $T^{-1/2}$ or $T^{-1/4}$.

general behavior $\sigma_{a.c.} \sim \omega^{\nu 1}$. So our samples had to be examined to see if their resemblance to the amorphous semiconductors included such a feature. It should be kept in mind that the goal is the comparative experimental behavior without regard - for the present - for the underlying mechanism or theory which is currently in considerable doubt.

By careful control over the compensation levels of a series of samples the expected frequency dependence was indeed observed. As can

be seen in Figure 4, increasing compensation not only lowers the conductivity (all measured at 4.2 K) but also gives rise to an increasing

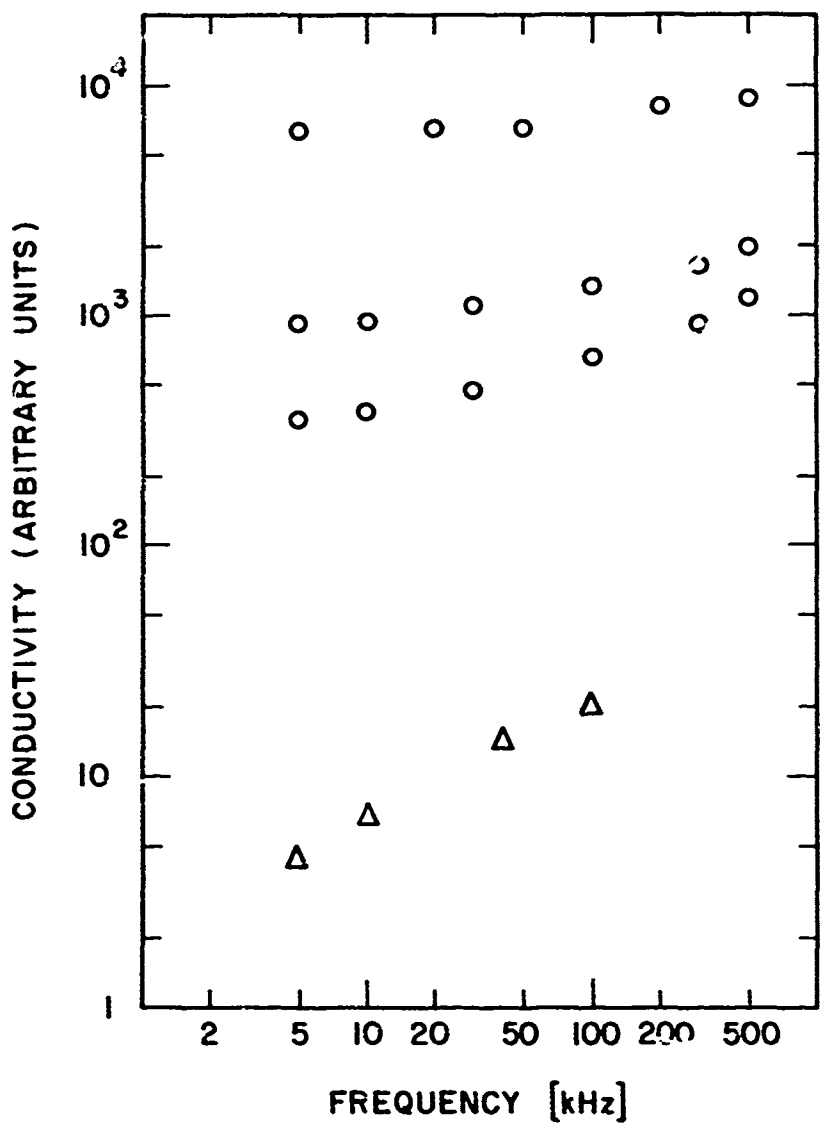

Figure 1-4. A.C. conductivity of a series of samples (at 4.2 K) for which lower conductivities correspond to closer compensation. The increasing frequency dependence thus created is also evident in the lower sets of data.

frequency dependence. When the compensation is extended sufficiently to produce a very high resistivity we see in Figure 1-5 the $\sigma \sim \omega^{\sim 1}$ of the usual type. That is, such behavior is usual for amorphous semiconductors and insulators. But it is very abnormal for GaAs to have a frequency dependence on its conductivity in this range of frequencies. Thus, we see another strong indication of the kind of localization effects characteristic of band tail states. In addition, we see clearly in Figure 1-4 that the onset of the frequency dependence associated generally with localized states is gradual as the deeper states of the tail are reached. This suggests that an abrupt mobility edge often used to describe the energy dependence of localization in a tail is not present in these materials. This is a major result of the present program and is supported strongly by the theoretical analysis of $\sigma(T)$ described in Section IV.

C. CURRENT-VOLTAGE RELATIONSHIPS

This aspect of the behavior of these materials has been the object of the most intensive recent work, both because the results are so interesting and because it has the closest bearing on possible switching applications. These measurements are continuing and being extended; those performed so far were limited to 4.2 K. To eliminate the effects of heating, pulsed voltages were used wherever possible, and the absence of thermal effects could be confirmed for all the data reported. At the lower voltages it was also possible to make dc measurements without significant heating so that the pulsed results could be checked. Furthermore, four probe samples were used for a number of experiments to exclude possible contact effects. These samples had natural geometrical limitations to the electric field strength attainable for the available voltages and thus could be used to confirm only the low-field portions of the conductivity, field strength curves. The higher-field portions were obtained from two-contact, wafer-like samples. The agreement of the results from the various methods shows that heating, contacts, or ac response played no important part in these results.

The data obtained so far are represented by the two curves in Figure 1-6 for wafer samples which are relatively high in conductivity but differ slightly in their compensation levels. It is apparent that the material is strongly non-ohmic at all observed voltages; the full equivalence of the negative polarity behavior taken together with the four-probe measurements confirm that these are the bulk properties. Therefore, these data can be converted to conductivity vs. field plots by the simple application of appropriate geometrical factors. This has been done for the same data shown in Figure 1-6, taking the total conductivity, not the differential. The results appear in Figure 1-7 as log σ vs. F because of the very wide range of conductivities. One curious result is that the lower conductivity of the more-compensated sample actually varies more rapidly with field in some ranges, causing the curves to cross. This is as yet unexplained.

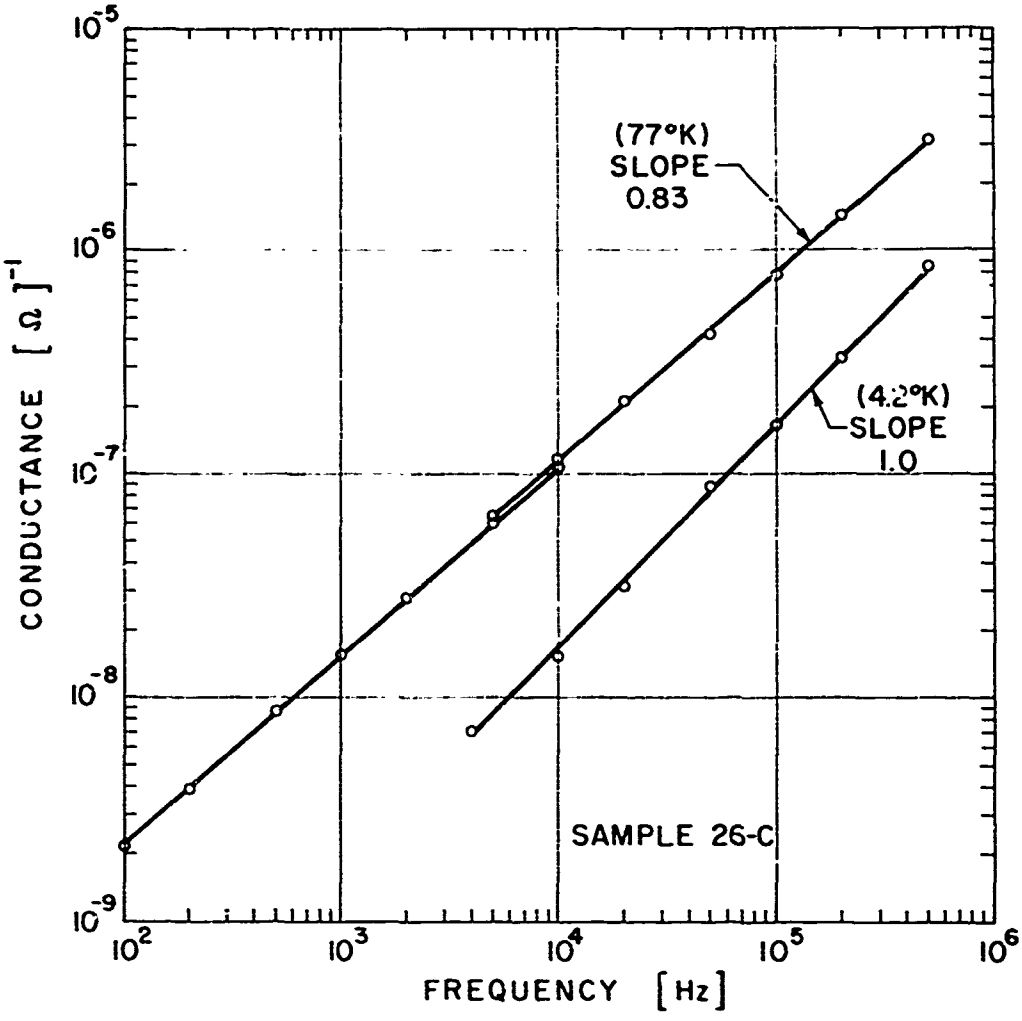

Figure 1-5. Frequency dependence of the conductivity for a very closely compensated sample.

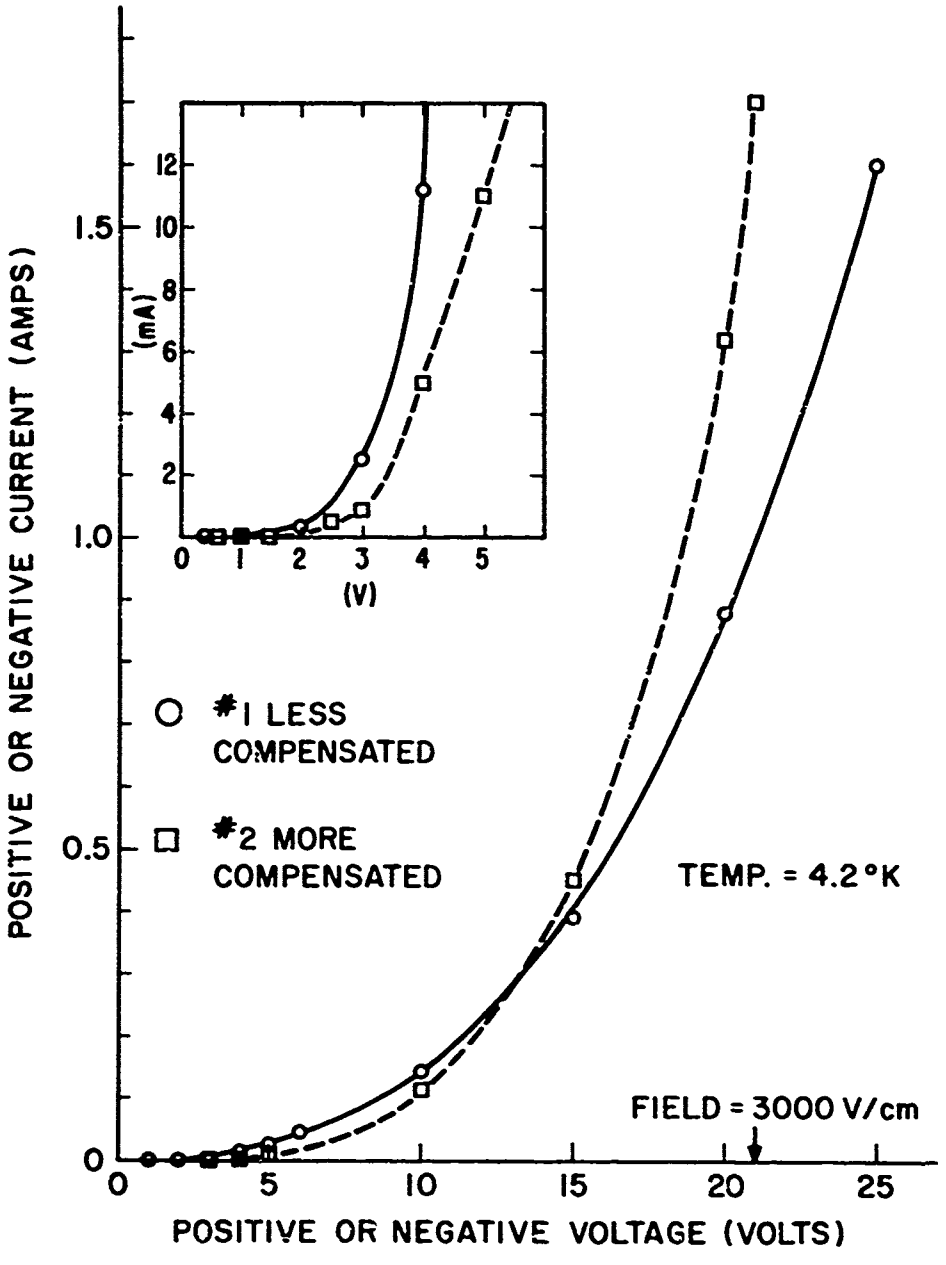

Figure 1-6. Current-voltage curves (at 4.2 K) of two relatively high-conductivity samples having slightly different compensation levels. There is no effect of polarity.

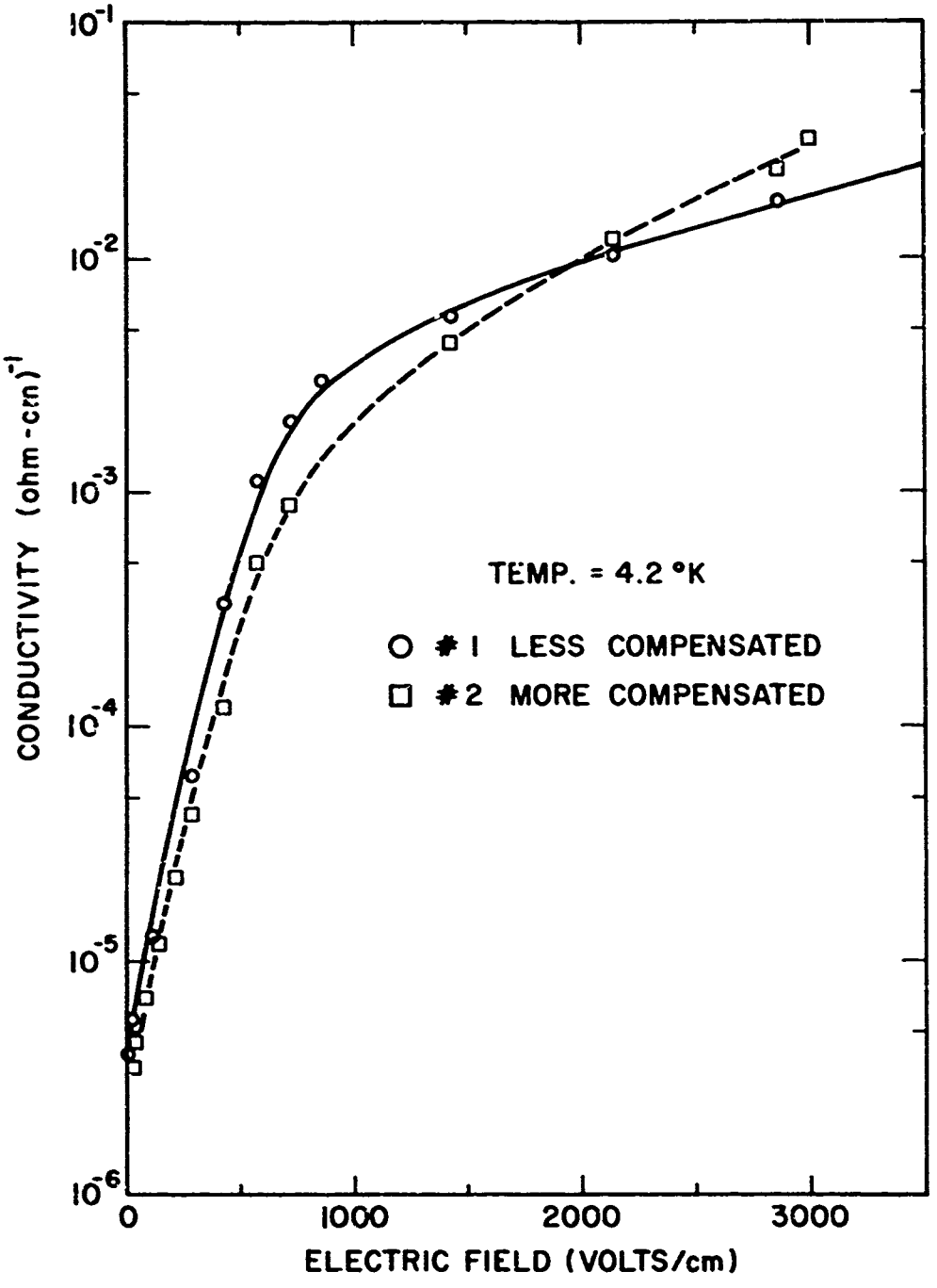

Figure 1-7. Electric field dependence of the conductivity using the same data as shown in Figure 1-6.

The primary result of these measurements, however, is the very strong field dependence of the conductivity. It can be seen that $\sigma \sim \exp F$ is a good approximation over at least three orders of magnitude of σ. Furthermore, this behavior extends to the lowest fields used -- $\sim$ 30 V/cm -- with no sign of levelling off. This is a remarkable result for the following reason. The very existence of a field-dependent conductivity in materials such as these indicates the presence of quasi-localized electrons which can be somehow freed by the field. For the very low fields to have an important effect, some of the electrons must be very weakly bound.

These current-voltage properties suggest possible applications of the materials in at least two fields. One is as a voltage surge arrestor which would protect electronic equipment from unexpected voltage surges by shunting the equipment with a resistance that could drop very rapidly in the presence of excess voltage. Although these samples do not have all the properties desired in such a device, the potentiality seems present.

The second possible application concerns one of the original possibilities that motivated this type of work - a negative-resistance device or switch. So far we have not observed negative resistance except when thermal influences seem present. But the great departures from ohmic behavior are promising, and considerable further work in this area appears warranted.

D. PHOTOCONDUCTIVITY

These measurements were initiated rather recently and extensive results are not yet available. The photoresponse at low temperatures has been found to have the following interesting features: A strong tail in the photoconductive spectral response (at low temperatures) exists for energies well below the normal gap energy. This tail requires moderately close compensation but is not very sensitive to the compensation level in this regime. Some preliminary optical absorption measurements have been made in this tail region to compare with the photoconductivity because this is normally a region of transparence. Hence, more information is needed about both of these optical properties. In addition, there is some evidence that these samples display an unusually strong temperature dependence of the photoconductive peak wavelength. At the present it is premature to judge the likelihood of useful photoconductive devices emerging from these materials. One related possibility, however, is a radiation detector using the bolometer effect of closely compensated thin films made this way.

E. MAGNETIC SUSCEPTIBILITY AND SPECIFIC HEAT

These measurements were attempted in collaboration with Dr. Donald Gubser of the Naval Research Laboratory as a result of some of the

theoretical work described in Section IV. There appears to exist in principle the possibility of directly measuring the density states as a function of energy in the tails if one of these measurements succeeds. Experimental limitations -- chiefly insufficient sample size -- have so far foiled these measurements. Further attempts are planned here.

F. THERMOELECTRIC POWER

The apparatus for this measurement was constructed but not actually put into use because the discovery of the remarkable current-voltage relations called for a greatly increased effort in that area. Nevertheless, the thermopower can be a useful supporting measurement which will be performed.

IV. THEORY

Because this program offers better opportunities for quantitative determination of properties of electronic energy band tails than any others known to us, there was a corresponding need for a larger theoretical basis for interpretation of the results. We have therefore developed an extension of the statistical behavior of solids to include band tails as an explicit case. This was performed first for an extrinsic material, like our samples, for which only one band tail plays a significant role. Then the intrinsic (2-band) case was treated and finally the combined case which transforms from extrinsic at low temperatures to intrinsic at high temperatures.

A. EXTRINSIC CASE

This portion was nearly completed at the beginning of this contract and is to be published as "Evidence for a Gradual Mobility Transition in Band Tails of Heavily Doped GaAs" in the Proceedings of the IV Intl. Conf. on Amorphous and Liquid Semiconductors[11]. Therefore, only the abstract is repeated here and the paper is reproduced as Appendix A.

> "An analysis is given of previously reported transport measurements in band tails of heavily doped, closely compensated GaAs. By use of a model density of states, the temperature dependence of the Fermi energy in the tail and the distribution of electrons among the states are found. Then the temperature dependence of the conductivity is calculated using the Kubo-Greenwood formula with a variable energy dependence of the mobility. A criterion is proposed for designating a mobility edge as sharp or not, and comparison with the experimental data indicates that in these samples the criterion is not met. Thus, the energy dependence of the mobility in the band tail is regarded as gradual."

B. INTRINSIC AND COMBINED EXTRINSIC-TO-INTRINSIC CASES

The statistical calculations on intrinsic materials were performed with the goal of applying the concepts developed for our band tail system to the problems of amorphous semiconductors which are widely regarded to be intrinsic. Comparison of the results of these calculations with published data for several amorphous semiconductors show a marked resemblance and again lead to the questioning of sharp mobility edges. Because the essential portions of the results of the intrinsic case were also published ("Statistical Properties of Disordered Semiconductors")[12] and are reproduced as Appendix B, only the abstract is given here.

"Basic statistical considerations are shown to imply pronounced effects on many properties of materials having energy band tails. For extrinsic cases a metal-like temperature dependence of the Fermi energy occurs; in consequence, a method is proposed for directly measuring the density of states in the tail. For intrinsic amorphous semiconductors, severe limitations are found for the inference of a sharp mobility edge from temperature-dependent conductivity data."

The second sentence of this abstract refers to the prediction that either the low-temperature specific heat or the Pauli susceptibility could furnish a quantitative measure of the density of states at the Fermi energy in a tail. This was the motivation for the attempts to make such measurements as mentioned in Section III-E.

The combined case has been calculated, showing how the Fermi energy moves from one band tail at low temperatures to the center of the pseudo-gap at high temperatures. The behavior is interesting but there is no example known to us in which a comparable experimental observation has been made. This may simply be a result of the lack of ability to identify such a situation but the application of this calculation must await such identification.

V. SUMMARY

This program has achieved a number of its goals in the study of disordered semiconductors. First is the ability to create materials with band tails that are tailored to our specifications and occupied to a precisely controllable extent. It has also been established that the interesting and unusual properties displayed by such materials are indeed attributable to band tail effects, not to the presence of particular kinds of impurities or defects. A variety of preparation processes has led to good reproducibility and control over these samples and to greatly improved electrical contacts for use on them.

The measured properties of these samples show many attractive features. One of the primary features for the present purposes is the very close similarity of the properties of these materials to those of amorphous semiconductors. Because the band tails here are smaller than those of the typical amorphous semiconductors, our measurements are generally at low temperature. But the knowledge gained this way might be extended to materials permitting higher-temperature operation and fabrication in thin films. In any event, the information obtained so far -- both experimental and theoretical -- is clearly relevant to the understanding of the electronic properties of amorphous semiconductors.

Another principal result is the demonstration, by combined experiment and theory, that sharp mobility edges are much less likely to prevail than is generally believed. We have several graphic indications of a gradual energy dependence of the mobility in the tail from a.c. conductivity, temperature dependence of the d.c. conductivity, and calculations compared to amorphous semiconductors.

The current-voltage relationships have exhibited some of the most unexpected and interesting behavior. The field dependence of the conductivity in these samples appears to be unique. Its continued sensitivity at very low fields is one of the most provocative results and promises to shed important light on the properties of band tails.

The various observed properties appear to lend themselves to several possible applications as in low-temperature thermometry, bolometric radiation detector, voltage surge arrestor, and general nonlinear electronic components.

REFERENCES

1. S. R. Ovshinsky, Phys. Rev. Lett. 21, 1450 (1968).
2. M. H. Cohen, H. Fritzsche, and S. R. Ovshinsky, Phys. Rev. Lett. 22, 1065 (1969). N. F. Mott, Phil. Mag. 22, (1970).
3. D. Redfield and R. S. Crandall, in *Proc. X. Intl. Conf. on Physics of Semiconductors,* edited by S. P. Keller, J. C. Hensel, and F. Stern; (U.S. National Tech. Information Serv., Springfield, Va., 1970) p. 574.
4. E. O. Kane, Phys. Rev. 131, 79 (1963); T. N. Morgan, Phys. Rev. 139, A343 (1965).
5. B. I. Halperin and M. Lax, Phys. Rev. 148, 722 (1966).
6. R. N. Hall and J. H. Racette, J. Appl. Phys. 35, 379 (1964).
7. H. J. Stein, J. Appl. Phys. 40, 5300 (1969).
8. N. F. Mott, Phil. Mag. 19, 835 (1969).
9. V. Ambegaokar, B. I. Halperin, and J. S. Langer, Phys. Rev. B4, 2612 (1971).
10. M. Morgan and P. Walley, Phil. Mag. 23, 661 (1971).
11. D. Redfield, J. Non-Crystalline Solids 8/9, 602 (1972). (See Appendix A.)
12. D. Redfield, Phys. Rev. Lett. 27, 730 (1971).

JOURNAL OF NON-CRYSTALLINE SOLIDS 8/9 (1972) 602-[redacted] Cohen

APPENDIX A

EVIDENCE FOR A GRADUAL MOBILITY TRANSITION IN BAND TAILS OF HEAVILY DOPED GaAs

DAVID REDFIELD

RCA Laboratories, Princeton, New Jersey 08540, U.S.A.

An analysis is given of previously reported transport measurements in band tails of heavily-doped, closely-compensated GaAs. By use of a model density of states, the temperature dependence of the Fermi energy in the tail and the distribution of electrons among the states are found. Then the temperature dependence of the conductivity is calculated using the Kubo–Greenwood formula with a variable energy dependence of the mobility. A criterion is proposed for designating a mobility edge as sharp or not and comparison with the experimental data indicates that in these samples the criterion is not met. Thus the energy dependence of the mobility in the band tail is regarded as "gradual".

One of the most severe problems in the study of electronic properties of disordered semiconductors is the absence of experimental knowledge of the energy band tails and their properties. For this reason we have developed a technique which permits control of band tails and their occupancy in heavily-doped, closely-compensated n-GaAs. A summary of this technique and results on the energy dependence of some of the transport properties have been published[1]). The temperature dependence of the conductivity of a series of four samples with Fermi energies progressively deeper in the tail[2]) is reproduced from ref. 1 in fig. 1a. The principal features of these data are: (a) the very large changes in temperature-sensitivity; and (b) the shapes of the curves which typically look nearly straight when they are steepest but concave upward for intermediate steepnesses (as for #1 in fig. 1a).

The present paper describes an analysis designed to provide a basis for interpreting the data of ref. 1. The conductivity data shown in fig. 1a are treated within the framework of the Kubo-Greenwood formula[3])

$$\sigma_{\mathrm{D.C.}} = e \int N(E)\, f(E)\, \mu(E)\, \mathrm{d}E, \tag{1}$$

where $N(E)$ is the density of states, $f(E)$ the Fermi function and $\mu(E)$ the energy-dependent mobility. A primary question is whether or not the results of fig. 1a are caused by an abrupt mobility edge of the type widely proposed for the band tails in amorphous semiconductors[3,4]). An alternate possibility

is a *gradual* reduction in mobility at deeper states of the tail so that low temperatures simply drop all electrons into states of lower – but non-zero – mobility. Thus the question becomes one of degree: how sharp is the energy dependences of the mobility?

To achieve even a semi-quantitative interpretation of any such data requires certain fundamental information such as the density of states function and the temperature dependence of Fermi energy $\zeta(T)$. Having those, various functions can be tried for $\mu(E)$ to fit the experimental results with eq. (1).

In heavily-doped, compensated semiconductors, various calculations[5,6] have shown that $N(E)$ is nearly Gaussian in the tail. This fact permits the use of a simple model for $N(E)$ consisting of a normal parabolic band joined to a Gaussian tail as shown in fig. 2a. Thus

$$N(E) = \begin{cases} A(E - E_c)^{\frac{1}{2}}, & E > E_j > E_c, \\ N_j \exp\left[-\left(\dfrac{E - E_j}{E_0}\right)^2\right], & E < E_j, \end{cases}$$

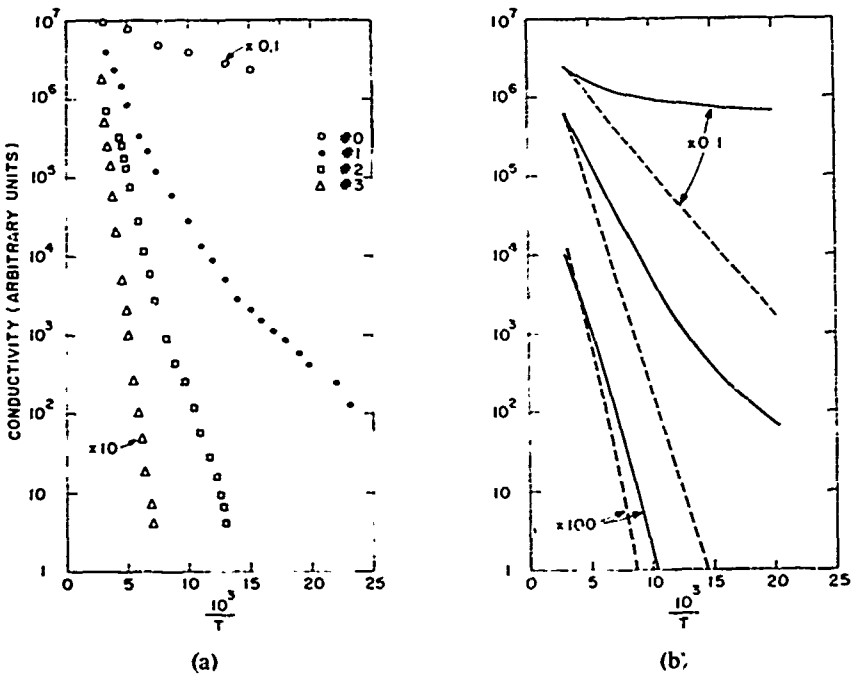

Fig. A-1. Temperature dependence of conductivity of heavily doped, closely compensated GaAs band tails. (a) Experimental data from ref. 1 for a series of samples having progressively closer compensation from #0 to #3. (b) Calculated conductivities from eq. (1) with the model density of states, E_0 = 0.06 eV and three values of ζ_0 to simulate the experimental data; dashed lines are for an ideal mobility edge ($E_\mu = 0$) and solid lines are for E_μ = 0.03 eV.

where E_j is the energy at which the two portions join, $N_j = A(E_j - E_c)^{\frac{1}{2}}$ for continuity and E_0 is the tail width parameter. Numerical calculations not based on this model have shown that the value of E_0 appropriate to the samples of fig. 1a is in the range of 0.03–0.06 eV [7]. With this model density of states thus fitted to more precise $N(E)$ functions, we have numerically computed the temperature dependence of the Fermi energy $\zeta(T)$ by the usual iterative method invoking particle conservation. The results of this calculation lead to a number of interesting and potentially useful conclusions which are discussed elsewhere [8].

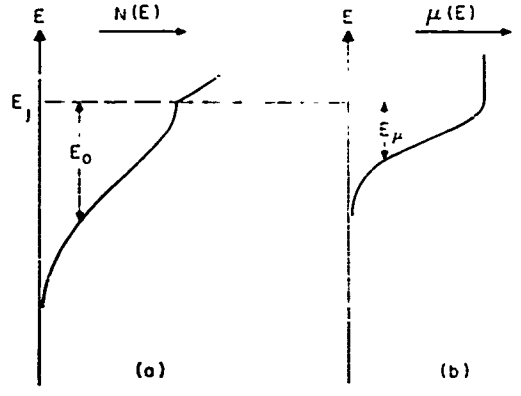

Fig. A-2. The model functions used in these calculations. (a) Density of states and (b) mobility plotted on the same energy scale. E_0 and E_μ are the respective width parameters ($E_\mu = 0$ corresponds to an ideal mobility edge).

Now having both $N(E)$ and $f(E, T)$ we can find the entire distribution of electrons over the states at any temperature. This is illustrated in fig. 3 using parameters appropriate to our samples. For evaluation of eq. (1) we have used a variety of functions to represent $\mu(E)$ and compared the results with those of fig. 1a. To permit an estimate of the sharpness of the mobility transition, we assign it a width E_μ as shown in fig. 2b. Since the precise shape of $\mu(E)$ is found to be less important than this width, we have generally used a Gaussian for $\mu(E)$ so that E_μ can be easily compared to E_0. In the absence of any other criterion for calling a mobility edge "sharp" we suggest the requirement that $E_\mu \ll E_0$.

After many computations of $\sigma(T)$ using eq. (1) with different trial values for E_μ to fit the experimental data, we find the following results: (1) The most suitable value for E_0 is about 0.06 eV. (2) The use of an ideal mobility edge (i.e. $E_\mu = 0$) is not capable of producing curved temperature dependences at any Fermi level position. This is shown by the dashed lines in fig. 1b for a set of values of the parameters thought to be appropriate for

the experimental samples. It should be noted that all other reasonable values of the parameters lead to the same conclusion. (3) Values of $E_\mu \simeq 0.03$ eV *are* capable of simulating the experimental curves fairly well in their shape and to some extent in their slopes as demonstrated by the solid lines in fig. 1b.

In view of the limitations imposed by the model functions used and by the number of parameters $[E_0, E_\mu, \zeta(0)]$ we do not claim to be able to fit quantitatively the experimental data. We *do* conclude, however, that an abrupt mobility edge cannot fit the conductivity data and is furthermore

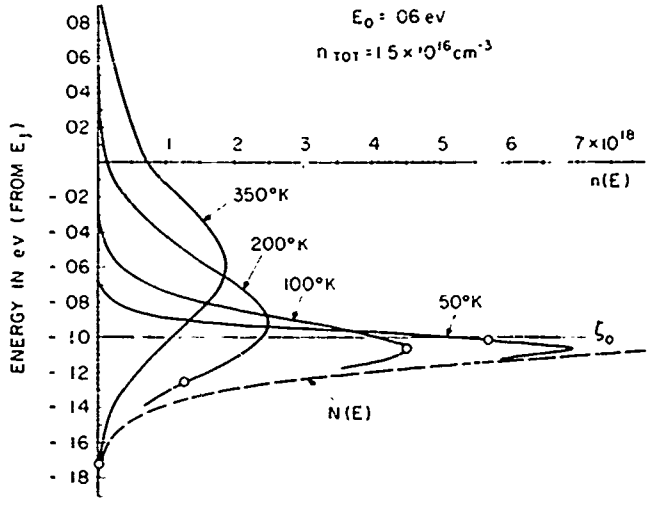

Fig. A-3. Distribution of electrons over the available energies at various temperatures. The dashed curve is the density of states tail. Open circles show the level of the Fermi energy for each curve. At $T = 0$ K the Fermi energy is at -0.1 eV as shown by horizontal line ζ_0.

inconsistent with the Hall effect data of ref. 1 on the same samples. The indicated value of $E_\mu = 0.03$ eV is half of the tail width; since this does not meet the criterion proposed above we regard this as a "gradual" mobility transition. In connection with this, it has also been shown that the inference of a sharp mobility gap from the apparent activated conductivity in amorphous semiconductors may also be unwarranted because of statistical effects not previously considered[8]).

References

1) D. Redfield and R. S. Crandall, in: *Proc. Tenth Conf. on the Physics of Semiconductors*, 1970 (U.S. Atomic Energy Commission, 1970) p. 574.

2) The Hall coefficient and Hall mobility data for these samples are not shown here, but support this interpretation.

3) M. H. Cohen, J. Non-Crystalline Solids **4** (1970) 391.

4) E. A. Davis and N. F. Mott, Phil. Mag. **22** (1970) 903.

5) B. I. Halperin and M. Lax, Phys. Rev. **148** (1966) 722;
T. N. Morgan, Phys. Rev. **139** (1965) A343.

6) F. Stern, Phys. Rev. **B3** (1971) 2636.

7) The author is indebted to F. Stern for these calculations.

8) David Redfield, Phys. Rev. Letters **27** (1971) 730.

APPENDIX B

VOLUME 27, NUMBER 11 PHYSICAL REVIEW LETTERS 13 SEPTEMBER 1971

Statistical Properties of Disordered Semiconductors*

David Redfield
RCA Laboratories, Princeton, New Jersey 08540
(Received 22 July 1971)

Basic statistical considerations are shown to imply pronounced effects on many properties of materials having energy-band tails. For extrinsic cases a metallike temperture dependence of the Fermi energy occurs; in consequence, a method is proposed for directly measuring the density of states in the tail. For intrinsic amorphous semiconductors, severe limitations are found for the inference of a sharp mobility edge from temperature-dependent conductivity data.

It is generally accepted that many of the interesting and potentially useful electronic properties of disordered semiconductors are associated with energy-band tails. These tails on the energy distribution of density of states create systems which are not conventional semiconductors, insulators, or metals. Therefore, the equilibrium statistical behavior cannot be obtained from any of the standard forms. This paper shows from calculations of this behavior for a simple model density of states that the statistical effects lead to new insights for both extrinsic and intrinsic cases. The essential conclusions appear to be independent of the details of the model.

The model used for the density of states was chosen as a simple, but fairly good, approximation to the several theoretical results appropriate to compensated semiconductors.[1-3] Each band edge is taken to be a normal parabolic band joined to a Gaussian tail as seen in Fig. 1(a). For a conduction band then

$$N(E)=\begin{cases}A(E-E_c)^{1/2}, & E>E_{jc}>E_c\\ N_j\exp\{-[(E-E_{jc})/E_0]^2\}, & E<E_{jc},\end{cases}$$

where E_{jc} is the energy at which the pieces join, $N_j=A(E_{jc}-E_c)^{1/2}$ for continuity, and E_0 is the (adjustable) tail-width parameter.

We treat first the extrinsic case, i.e., one in which only one band plays a significant role because of an excess of one type of carrier (electrons for definiteness). The initial need, before any of the physical properties can be computed, is to evaluate the temperature dependence of the Fermi energy. This has been done numerically by the usual method of particle conservation. The results shown in Fig. 2 are representative of heavily doped, closely compensated semiconductors. A primary result is that the Fermi en-

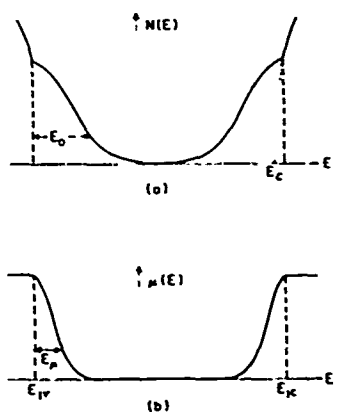

FIG. B-1. The model functions used in these calculations. (a) Density of states and (b) mobility on the same energy scale. E_0 and E_μ are the respective width parameters. $E_\mu=0$ corresponds to an ideal mobility edge.

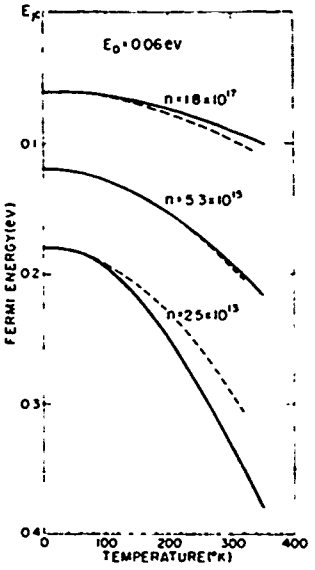

FIG. B-2. Computed Fermi energy (solid curves) in the band tail as a function of temperature for an n-type extrinsic semiconductor with three values of the excess electron concentration. Dashed curves are the metallic approximation, Eq. (1).

ergy ζ is *quantitatively* described, particularly at low temperatures, by the customary approximation used in metals,

$$\zeta = \zeta_0 - \tfrac{1}{6}\pi^2(kT)^2[\partial \ln N(E)/\partial E]_{E=\zeta_0}, \quad (1)$$

where ζ_0 is the value at $T = 0$ K. This is a somewhat unexpected result in view of the strong energy dependence of the density of states in the region of interest and the large range over which the Fermi energy may vary. One important consequence of this result is that some of the low-temperature equilibrium properties should be quasimetallic. For example, the validity of Eq. (1) implies that there should be a linear temperature dependence of the specific heat at low temperatures:

$$C = \tfrac{1}{3}\pi^2 k^2 T N(\zeta_0). \quad (2)$$

Because $N(\zeta_0)$ is small compared to its value in metals, this should be a small effect and be measurable only at very low temperatures. Nevertheless, just such an effect has been reported[4] recently for several glassy materials below 1 K. Using any of the values reported in Ref. 4 for C and a reasonable band-tail width, one finds an estimated total carrier concentration of 10^{17}–10^{18} cm^{-3} which is consistent with the value measured by magnetic susceptibility for amorphous As_2S_3.[5] To support this suggestion that electrons in band-tail states are responsible for the specific heat observations, it is also necessary to invoke the localized character of such states[6] to explain the low electrical conductivity and the lack of sensitivity of C to magnetic fields.[4] It must be stressed that if this suggestion is correct, it offers the first means of experimentally measuring $N(E)$ using Eq. (2). By similar arguments, the Pauli spin susceptibility at low temperatures should also give a direct measure of $N(E)$.

Having the density of states and $\zeta(T)$, it is then possible to calculate the electrical conductivity as a function of temperature based on the Kubo-Greenwood formula,[6]

$$\sigma_{dc} = \int N(E) f(E) \mu(E)\, dE, \quad (3)$$

by simply choosing any function for the conductivity mobility $\mu(E)$. The results of this procedure will be given for the intrinsic case below. For an extrinsic case it has been shown[7] that an *abrupt* mobility edge does not well describe experimental results in heavily doped, closely compensated GaAs.

We next consider the intrinsic case in terms which might reasonably be compared with some amorphous semiconductors. We choose a pseudogap $E_{jc} - E_{jv}$ of 1 eV and density-of-states effective masses equal to the free-electron mass for both bands. Thus the Fermi energy is fixed at 0.5-eV separation from each E_j. For use in Eq. (3) the mobility function is taken to be constant in each "normal-band" range of energies and to decrease in each tail with a width parameter E_μ as shown in Fig. 1(b). The functional form of $\mu(E)$ in the tails was chosen to be Gaussian for convenience in comparing E_μ with E_0, not because it has any physical significance. (Other functions were tried with qualitatively the same results.)

A representative set of results of the computation of Eq. (3) for this case appears in Fig. 3. There are two principal conclusions from these results. The first is that the appearance of "activated" conductivity over many decades and with a reasonable activation energy does not *necessarily* require an abrupt mobility edge; we have taken $E_0 = 0.2$ eV, and it may be seen that E_μ can be as large as 0.1 eV without seriously altering such an appearance.[8] The choice of $E_0 = 0.2$ eV

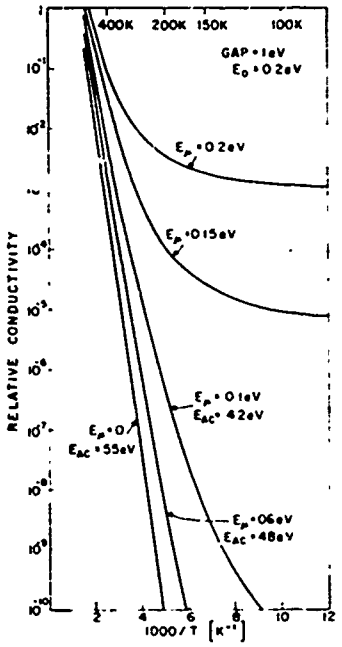

FIG. B-3. Computed conductivity as a function of reciprocal temperature from Eq. (3). The values of parameters E_0 and E_μ and the pseudogap are explained in the text. $E_\mu = 0$ corresponds to an ideal mobility gap. E_{AC} is the apparent activation energy deduced from the upper portions of the curves. See Ref. 12 for comparable experimental results.

is quite arbitrary in view of the wide disagreement as to just how broad the tails are,[6,10] but it is a conservative choice for the present purposes. It was made because it produces ~10^{19} states/eV cm^3 at the gap center, one of the values most often quoted.[11]

There are, of course, strong theoretical arguments for very low mobilities deep in band tails. The immediate questions are these: How abrupt is the mobility transition, and do the available experimental results permit conclusions to be drawn concerning this abruptness? The present results indicate that the appearance of activated conductivity in amorphous semiconductors does not permit conclusions about the abruptness to be drawn directly from the Kubo-Greenwood relation. The reason for this is that the two unknown functions of energy in Eq. (3), the density of states and mobility, enter in completely symmetric ways for the intrinsic case.[8] The present calculation shows statistically that these can combine in ways which simulate activated conductivity even in the absence of a physically well-defined activation energy in either the density of states or the mobility. Thus the narrower the band tail, the broader can be the mobility transition for any fixed conductivity plot.

The second conclusion from the results shown in Fig. 3 is that the existence of substantial conduction within the tails gives rise to what *appears* to be extrinsic low-temperature conductivity with a much weaker temperature dependence than the "intrinsic" behavior. In this regard, a series of experimental curves like those of Fig. 3 has been reported for a four-component semiconducting glass with various annealings.[12] We note that the leveling off in low-temperature conductivity should not occur in a system having an ideal mobility gap ($E_\mu = 0$). Conversely, it now appears unnecessary to invoke some *ad hoc* additional model such as a density-of-states peak at the gap center[10] to explain low-temperature conductivity having a very weak temperature dependence.

Finally, it should be remarked that this discussion has considered only the most elementary processes; undoubtedly, other effects will have to be included for a quantitative description of conductivity. For example, a temperature dependence of the mobility may well be important, although the qualitative conclusions presented here should not be seriously affected.

---

*Work supported in part by the Office of Naval Research under Contract No. N00014-71-C-0371.

[1]B. I. Halperin and M. Lax, Phys. Rev. 148, 722 (1966).
[2]T. N. Morgan, Phys. Rev. 139, A343 (1965).
[3]F. Stern, Phys. Rev. B 3, 2636 (1971), and private communication.
[4]R. B. Stephens, R. C. Zeller, and R. O. Pohl, Bull. Amer. Phys. Soc. 16, 377 (1971).
[5]J. Tauc, A. Menth, and D. L. Wood, Phys. Rev. Lett. 25, 749 (1970).
[6]M. H. Cohen, J. Non-Cryst. Solids 4, 391 (1970).
[7]D. Redfield, in Proceedings of the Fourth International Conference on Liquid and Amorphous Semiconductors, Ann Arbor, Michigan, 1971 (to be published).
[8]This symmetry does not extend to the extrinsic case in which $n(E)$ has the additional role of determining $\tau(T)$.
[9]The values $E_0 = 0.2$ eV and $E_\mu = 0.1$ eV are those used in Fig. 1 with a pseudogap of 1 eV.
[10]E. A. Davis and N. F. Mott, Phil. Mag. 22, 903 (1970).
[11]E. A. Fagen and H. Fritzsche, J. Non-Cryst. Solids 4, 480 (1970).
[12]E. A. Fagen and H. Fritzsche, J. Non-Cryst. Solids 2, 170 (1970).

PART 2

TRANSITION METAL OXIDES

by

Isaac Balberg

PART 2 - TRANSITION METAL OXIDES

I. INTRODUCTION

The main purpose of the present study was to get better knowledge and understanding of the electronic properties of materials that exhibit the metal-to-insulator transition and for which we have previously induced optical[1,2] as well as electrical[3,4] switching. Two other objectives were to evaluate practical applications of the switching effects and to examine theoretically and experimentally the mechanism suggested for "polaron switching"[5].

The materials studied were magnetite (Fe_3O_4), vanadium dioxide (VO_2), and oxygen-deficient rutile (TiO_{2-x}). The first two were chosen because they are the only two materials that have satisfactory switching characteristics and the rutile because it seems to be the only material in which polarons are believed to exist.

Since all the above materials are not commercially available in the forms needed for the present study, the main effort in this work was to grow crystals and prepare thin films of these materials, and to characterize them. The effects of doping, alloying, and deviation from stoichiometry on the metal-insulator transition were studied.

Very many experimental techniques were used for the study: (1) electrical transport, (2) high electric field effects, (3) tunneling, (4) uniaxial pressure effect on the conductivity, (5) optical reflectivity and transmission, (6) cathodoluminescence, (7) x-ray defraction, (8) specific heat, and (9) Raman scattering. Two possible applications of VO_2 were carefully studied: optical holographic storage and electron beam recording.

The main achievement of the present study is the first consistent understanding of the electronic structure of magnetite. Many other results confirm or contradict "accepted" results reported in the literature. Our results clarify the experimental situation, raise questions, and suggest further research in the present field.

The report is divided according to the three materials studied (Fe_3O_4, VO_2, and TiO_{2-x}), since in each of these materials different problems are present and different state of the art is encountered. Only general information on these materials is included here; further data can be found in known review papers[6,7]. For each material we shall first discuss the material preparation techniques, then the experimental results; and finally, we shall summarize them and reach conclusions based on the data.

This study could not have taken place without the close collaboration with: B. Abeles, S. R. Bolin, L. R. Friedman, J. I. Pankove, H. L. Pinch, E. B. Priestly, W. R. Roach, and L. J. Vieland, all members of the Technical Staff at RCA Laboratories. The technical assistance for the study was provided by Y. Arie, J. E. Berkeyheiser, Jr., and S. T. Opresko.

II. MAGNETITE

Magnetite is a ferrimagnet with T_N = 850 K. At room temperature it has a cubic inverse spinel structure, and at T_V = 120 K it goes through crystallographic as well as an "insulator-to-metal" transition. The electronic structure of this material was unknown before this study. The mechanism of the transition, in view of this study, seems to be more complicated than previously suggested.

A. CRYSTAL GROWTH OF Fe_3O_4

For the present study, crystals of pure and doped Fe_3O_4 were grown by closed-tube vapor transport[8,9]. The chemical transport was carried out in sealed fused silica tubes, in a gradient furnace (1000°-850°C) with HCl as the carrier gas. The crystals were grown at the cooler end of the tube and were obtained as small regular octahedra, 1 to 5 mm long across the apeces, and with smooth reflecting surfaces. However, the Fe_3O_4 attacked the inner walls of the silica tubes at the point of attachment, which tended to limit the crystal size and perfection. The source material for the crystal growth was prepared by the reduction of Fe_2O_3, i.e., by heating the Fe_2O_3 in a 2 to 1 gas mixture of CO_2 and CO at 650°C for 16 hours. The reduction $3Fe_2O_3 + CO \rightarrow 2Fe_3O_4 + CO_2$ was stoichiometric to within less than 0.1%. Chemical analysis of the as-grown crystals indicated that the Fe_2O_3/FeO ratio was 0.94. Improvement of the Fe_3O_4 crystal stoichiometry was effected by heating the crystals under the same oxygen partial pressure (CO_2/CO gas flows) and temperature used to prepare the stoichiometric Fe_3O_4 powder. However, because the as-grown crystals may vary considerably in size and their off-stoichiometry, the final state of stoichiometry of the heat-treated crystals also may vary. In all cases, it is believed that the chemical stoichiometry of the crystals is closer to the theoretical value as a result of the post-growth heat treatment.

Doped crystals of composition $M_xFe_{3-x}O_x$ (where M is either Ni or Co) were also grown by the same methods. Chemical analysis by flame atomic absorption of crystals made with starting materials of x = 0.03 showed that x = 0.028 for Co and x = 0.035 for Ni. The degree of factionation of the dopant was small and thus the nominal concentration of dopant is used to describe the crystals.

B. PREPARATION OF THIN Fe_3O_4 FILMS

For the optical measurements complementry to the results obtained on single crystals, thin (2 μm) Fe_3O_4 films were prepared. This was done by argon ion sputtering of iron onto Corning type 0221 glass. The iron films were oxidized to Fe_2O_3 by heating in a slow oxygen flow at 300°C for 2 hours. The Fe_2O_3 films were then reduced to Fe_3O_4 by heating to

380°C in the CO_2/CO gas mixture used to prepare Fe_3O_4 for crystal growth (see above). The oxidation and reduction steps were identified by x-ray diffraction. The Fe_3O_4 films were found to be single-phase, highly oriented, and polycrystalline. The orientation was such that the [110] axis was perpendicular to the substrate.

C. ELECTRICAL CONDUCTIVITY OF Fe_3O_4 CRYSTALS

Four-probe conductivity measurements were carried out by cooling or warming the crystals in the temperature range 4.2 - 350 K. Electrical ohmic contacts were made by smearing In-Hg amalgam on the desired surface and bonding to it with an In solder. Typical results of the temperature dependence of the conductivity σ are shown in Figure 2-1. The room-temperature value of the conductivity was typically 250 $(ohm\text{-}cm)^{-1}$, the

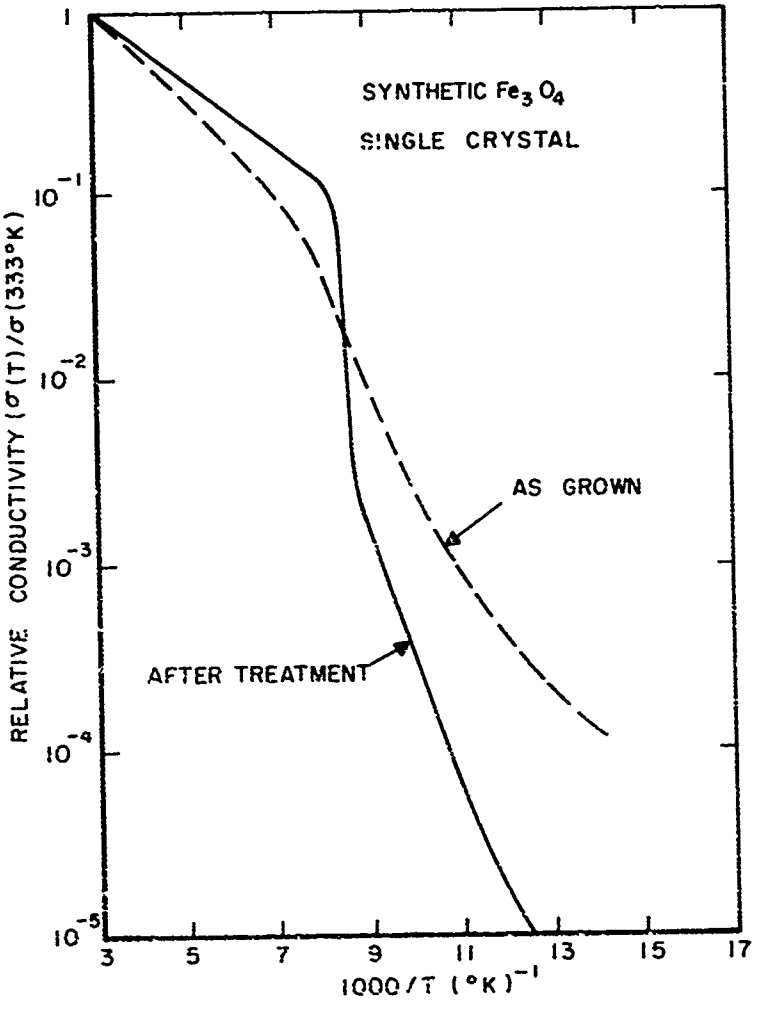

Figure 2-1. Temperature dependence of the conductivity before and after heating the crystal in a gas mixture of CO_2/CO.

value reported in the literature[6]. In this figure it is clearly demonstrated that the heating of the as-grown crystals in the 2:1 CO_2/CO mixture has three effects: (1) It sharpens the conductivity jump; (2) it increases the activation energy below T_V, up to the "intrinsic" value[10] of 0.15 eV; and (3) the transition temperature increases which, according to the pioneering work of Verwey[11], indicates an improvement of the stoichometry of the material. Such treatments of natural magnetite crystals (which are doped with ∿1% Ti and 0.15% Zn) has the same effect. This is shown in Figure 2-2. The

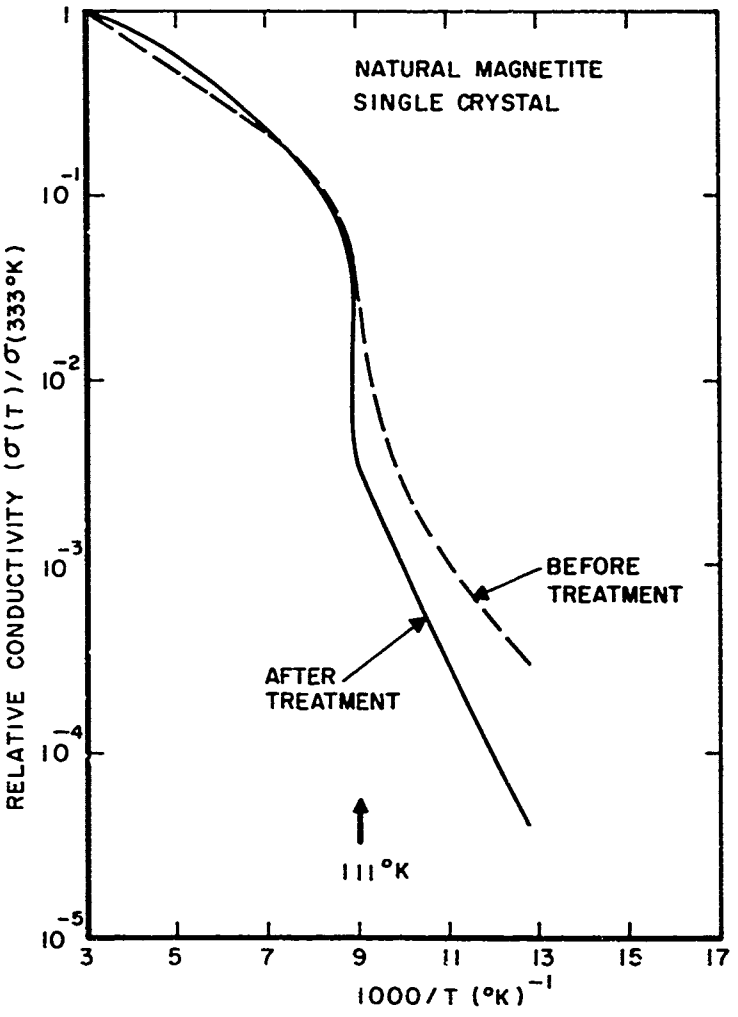

Figure 2-2. Temperature dependence of the conductivity of a natural single crystal after heating in a gas mixture of CO_2/CO.

effectiveness of the CO_2/CO treatment in improving the stoichiometry as well as the correctness of the above-mentioned indications are demonstrated in Figure 2-3. Two crystals that originally had the same

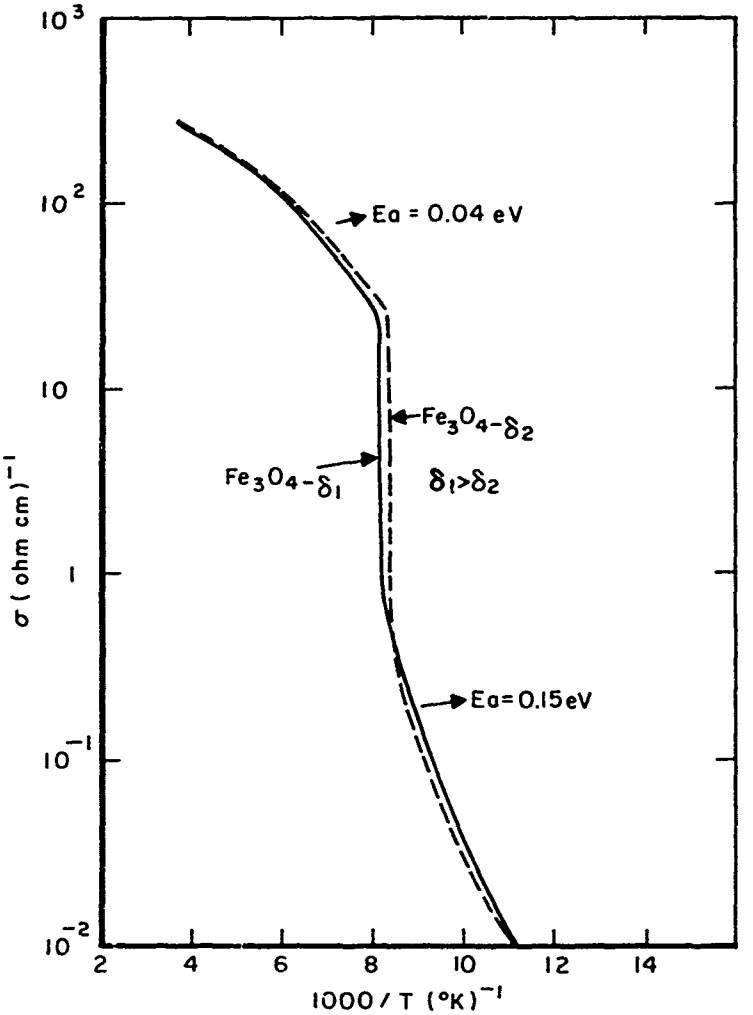

Figure 2-3. Temperature dependence of the conductivity of synthetic single crystal after treatment in two gas mixtures with different CO_2/CO ratio.

transition temperature differed after being heated in different CO_2/CO ratios. In one case this ratio was larger than 2 ($Fe_3O_4-\delta_1$) and in the other smaller than 2 ($Fe_3O_4-\delta_2$). The transition temperature has changed while the activation energy still has the intrinsic value of 0.15 eV. This is the first study of the effect of stoichiometry since the 1941 work of Verwey[11].

The other effect studied is that of doping Fe_3O_4 with Ni or Co, the ions of which occupy the octahedral sites (as expected from the site preference stabilization energies of Ni^{+2} and Co^{+2}). Even after the CO_2/CO treatment the transition temperature remains appreciably lower than that of the "pure" material, and the activation energy of the low temperature phase remains smaller than the "intrinsic" value. For impurity concentrations higher than 2.5% one finds that the metallic phase is maintained down to very low temperatures. The effects of doping and stoichiometry are shown in Figure 2-4. Also shown is the effect of gross deviation from stoichiometry when an α-Fe_2O_3 phase is present. The behavior then is of an "insulating" phase up to 350 K. Previous measurements on Ni- and Co-doped Fe_3O_4 were quoted by Miles et al.[12], but from their $\sigma(T)$ dependence it appears that stoichiometry played a more decisive roll than the doping. While our results agree qualitatively with theirs, their quantitative results do not seem to be reliable. In all the measurements no hysteresis was observed in the $\sigma(T)$ curve around T_V in accord with previously reported results and in contrast with the results in other first-order metal to insulator transitions[6].

For the measurements to be reported below, we have used natural magnetite and Fe_3O_4 films for the optical measurements, and CO_2/CO-treated synthetic crystals for the specific-heat measurements. For the x-ray measurements we have used synthetic as well as natural magnetite crystals (CO_2/CO-treated and untreated) to establish the generality of the results obtained.

D. OPTICAL MEASUREMENTS ON Fe_3O_4

Optical transmission measurements in the spectral range $0.15 \leq h\nu \leq 0.75$ eV were made on natural magnetite single crystals and in the spectral range $0.5 \leq h\nu \leq 3.5$ eV on thin (2 μm) Fe_3O_4 film. Taking into account the reflectivity of Fe_3O_4 (measured separately) we found the photon energy, $h\nu$, dependence of the absorption coefficient α in the above-mentioned spectral ranges. The same spectra were found both at 300 K and 77 K. This indicates absorption edges at 0.3 eV and at 2 eV and a plateau between 2.8 and 3.5 eV. These results are shown in Figure 2-5.

Cathodoluminescence studies of the crystals have produced complementary information. A peak at 2.6 eV and a shoulder at 3.2 eV were found in these spectra. These results combined with the optical data and available soft x-ray data have enabled us to present a semiquantitative band structure of Fe_3O_4 and to explain the previous transport data. The details of the measurements and their interpretation are given in Appendix C and Appendix D. The main consequences are presented at the end of this Section.

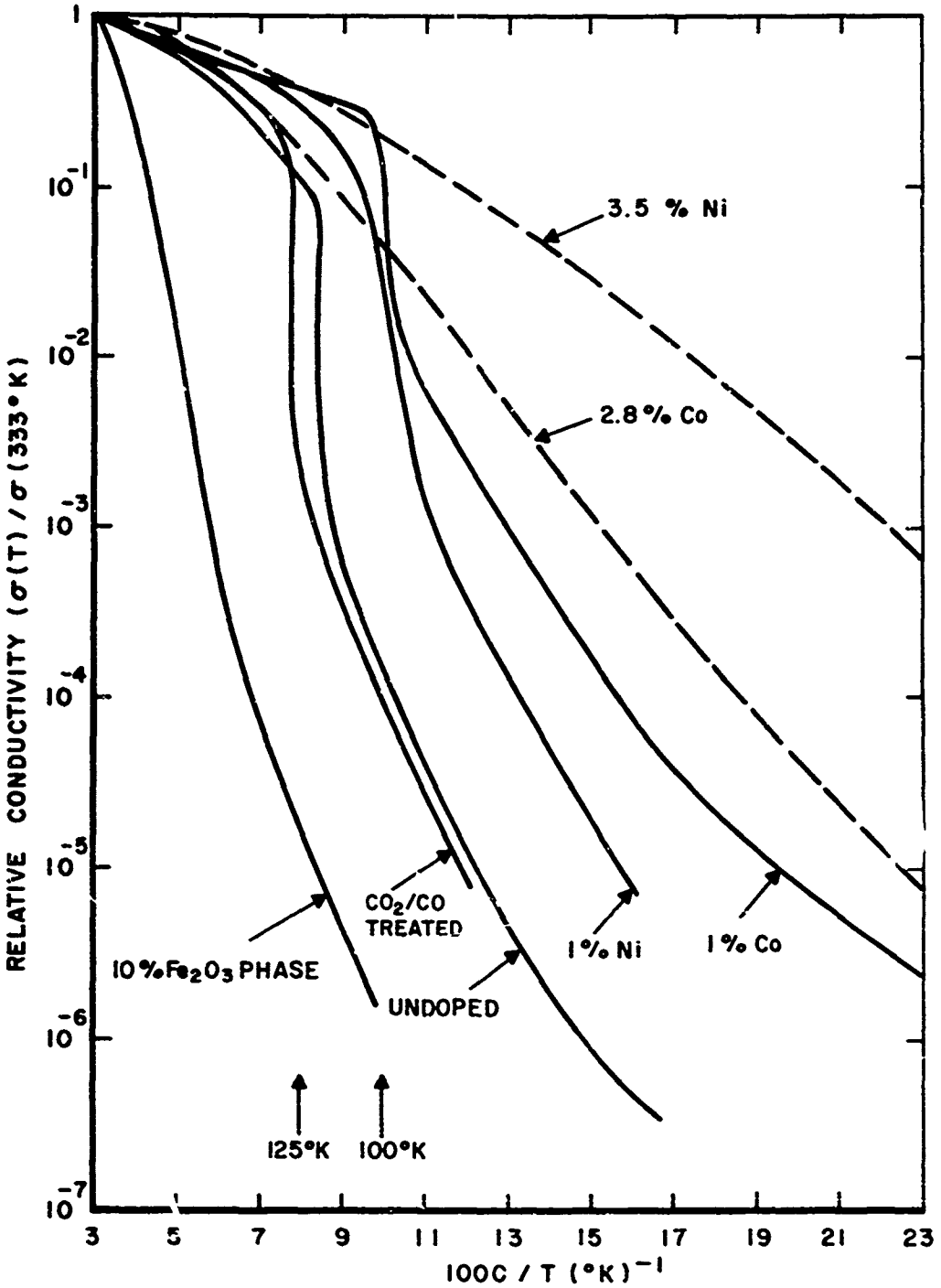

Figure 2-4. Temperature dependence of the conductivity of synthetic single crystals with various dopants and stoichiometries.

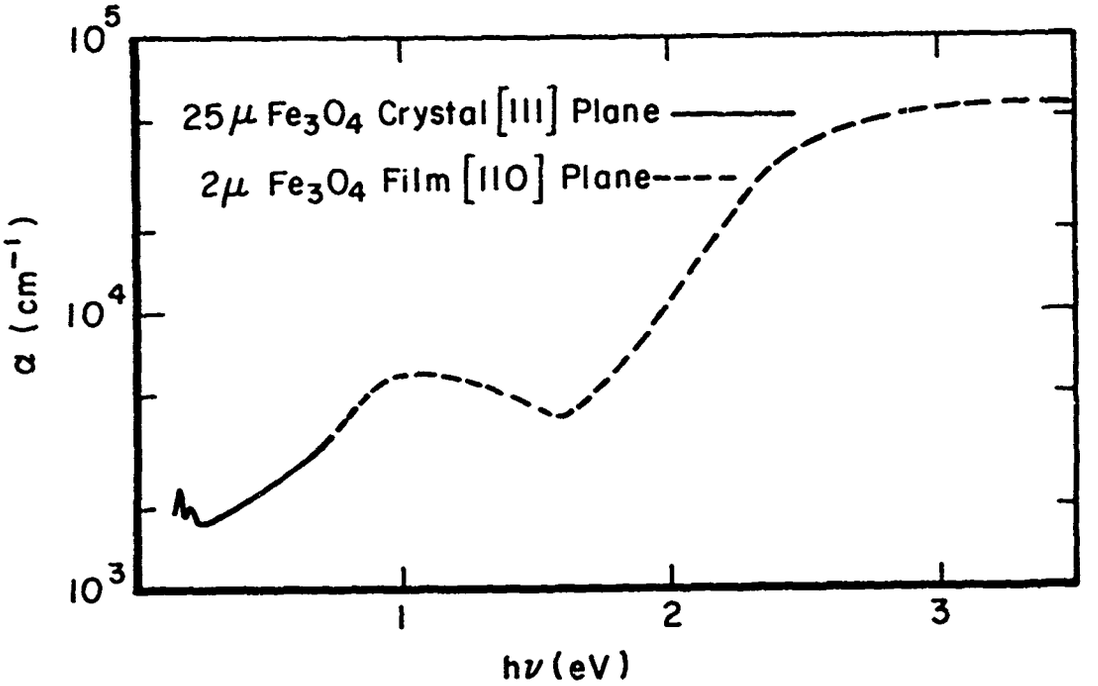

Figure 2-5. Optical transmission of natural Fe_3O_4 crystal and polycrystalline Fe_3O_4 film.

E. SPECIFIC HEAT OF Fe_3O_4

The specific heat of a collection of several small synthetic crystals of Fe_3O_4 was measured by heat pulse calorimetry. The thermometer and pulse heater were fabricated from a thin Si film deposited on a sapphire substrate. By varying the doping and thickness of the Si film, material having a temperature-dependent resistivity suitable for resistance thermometry can be deposited. Because of the small thermal mass of the sapphire substrate (and negligible mass of Si), samples weighing less than 200 mg were readily measured. The Si thermometer was calibrated against Pt in a separate experiment. Crystals having smooth facets were bonded to the sapphire on the side opposite from the Si, with a small amount of cement. Thermal *time* constants of a few seconds were formed, and data were obtainable with pulse heights of 50 mK.

The results are shown in Figure 2-6. We interpret the data as being consistent with a smeared first-order transition. The measured peak height is independent of pulse height, indicating the absence of a singularity of any kind. We think that the shoulder on the low T side of the peak is due to sample inhomogeneities, since crystals from various growth lots were measured together ($\sim$10 small crystals/sample). The

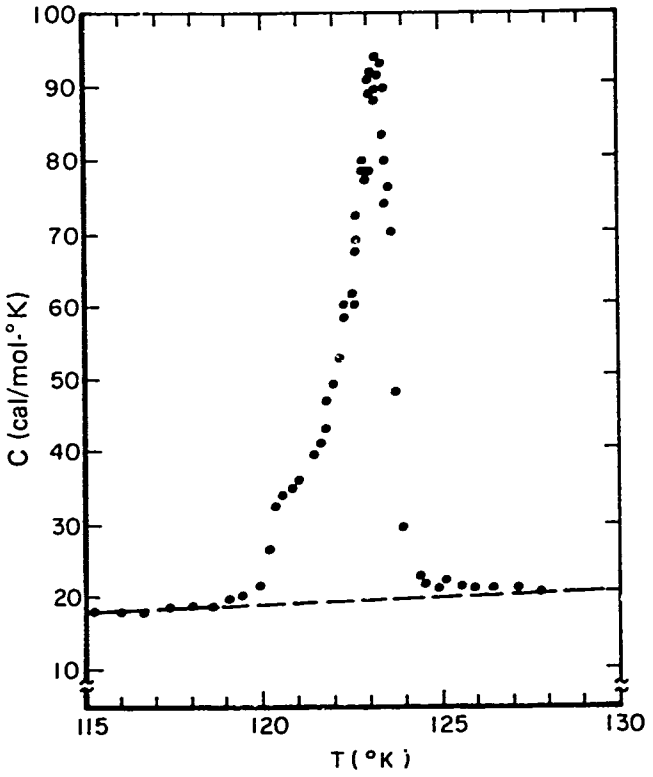

Figure 2-6. Specific heat as a function of temperature in the transition region of Fe_3O_4.

integrated area under the curve is 608 joules/mole, within 20% of the value obtained on natural crystal[13], although the transition width reported here is an order of magnitude smaller and sharper than any peak reported thus far. This latent heat corresponds to a change of entropy of 0.29 k_B per octahedral site in accord with the value quoted by Anderson[14].

F. X-RAY ANALYSIS OF Fe_3O_4

X-ray studies of the transformation were carried out on natural and synthetic single crystals using simple crystal diffractometry techniques. The low-temperature symmetry was determined by studying the splitting in (100), (110), and (111) type reflections accompanying the transformation. With regard to both peak positions and multiplicity, the reflections were found to be inconsistent with the assumption of orthorhombic symmetry, which is the accepted[6], low-temperature phase symmetry of Fe_3O_4. Based on the results for (110) and (111) types, which are found to split into a doublet of equal intensity ratio and

a doublet of 3/1 ratio respectively, the symmetry can be assigned unambiguously as rhombohedral. This is confirmed for (100) types, which remain unsplit, although peak broadening associated with crystallographic domain formation might obscure a small uniaxial component. We find the rhombohedral angle to be $\beta = 59° 48.5' \pm 0.2'$, thus confirming the earliest work on the phase transition on powders by Rooksby and Willis[15], who found $\beta = 59° 47.5'$.

As the temperature is lowered through the transition, the intensity of the cubic line [say (111)] decreases sharply near T_V, while the split peaks grow. No evidence for values of β significantly different from that given above were observed, i.e., the transition is clearly first order. However, the volume fraction of rhombohedral phase grows smoothly over a few degrees below the onset of the transformation. Thus, a sharp peak in the specific heat, *without* a latent heat, is understandable. Simultaneous measurements of the decrease of the cubic line intensity and the electrical resistivity have shown that there is no hysteresis associated with the transition and that indeed (as expected, but not reported so far) both the structural change and the conductivity jump represent the same transition.

G. UNIAXIAL PRESSURE MEASUREMENTS

Whereas the effect of pressure on the transition in the vanadi oxides with the metal-to-insulator transition has been extensively st ... for Fe_3O_4 only hydrostatic pressure measurements have been reported[16]. The experimental data of these measurements were not given, and it is not clear how sharp the transition was or how the transition temperature is identified. The reported results were that T_V shifts with the pressure P at the rate of $dT_V/dP = -0.5$ K/kbar over a 20 K range. This is consistent with the increase in the volume of the unit cell upon cooling through T_V.

In view of the above x-ray data it would have been expected that pulling along the [111] axis will cause an increase in T_V. Unfortunately, such an experiment is quite complicated to perform. On the other hand, the effect of pressure along one of the [111] directions will be to choose one of the other [111] directions as the elongated axis. Since only one of the other three [111] axes should be elongated, the transition is also expected to be broadened by the uniaxial pressure as in the case[17] of VO_2 (see below).

For the measurement a special system utilizing a deep stick with a piston was constructed. The uniaxial pressure was provided by gas pressure on the piston. With this system pressures of 50 kbar with a sample of 1-mm^2 area can easily be obtained. For the present study, however, we have only used pressures up to 2 kbar. With higher pressure it becomes hard to identify the T_V point, although qualitatively it is clearly shifted to higher temperatures.

In the results shown in Figure 2-7 we see that the behavior is consistent with the expectations. This is the first observation of a uniaxial pressure that increases the metal-to-insulator T_V. Quantitatively,

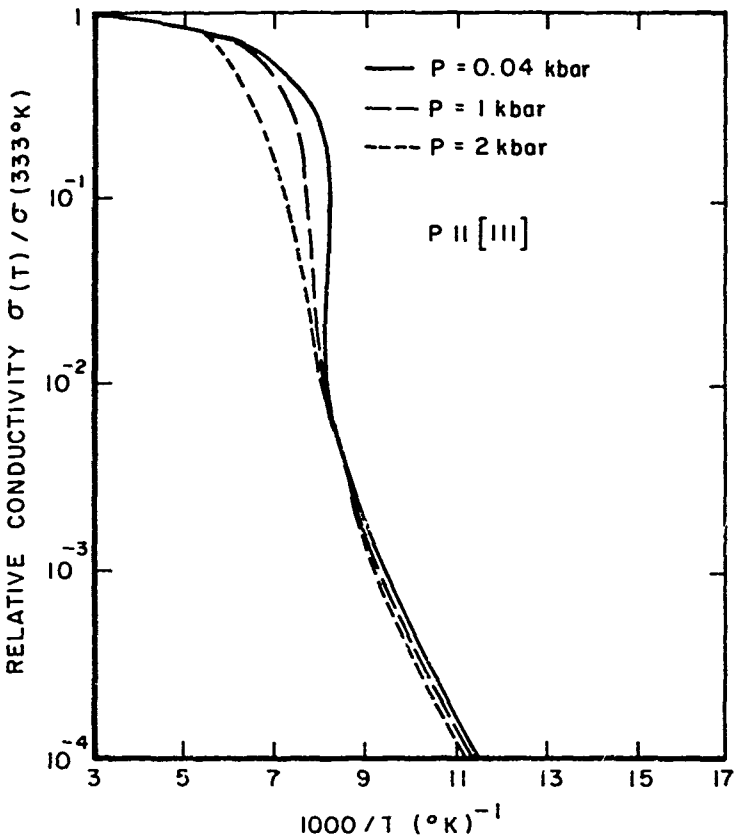

Figure 2-7. Temperature dependence of the conductivity of a synthetic single crystal under different uniaxial pressures.

the effect is very large. Although it depends on the choice of T_V, it is clearly of the order of $dT_V/dP \approx 10$ K/kbar. The calculated value, on the basis of pulling the [111] axis and the reported elastic constants[18], is 8.6 K/kbar.

H. SUMMARY AND CONCLUSIONS

The optical and cathodoluminescence data discussed above indicate optical transitions that correspond to transitions with photon energies of 0.3, 2, 2.6, and 3.2 eV. As shown in detail in Appendix C these yield

a consistent semiquantitative band structure that is based on the crystal field splitting of the octahedral sites. The atomic iron 3d level is split by the difference in exchange interaction to spin-down $3d_\alpha$(Fe) levels and to spin-up $3d_\beta$(Fe) levels. In the crystal each of these fivefold degenerate levels is further split by the crystal field. In the octahedral sites this splitting is to a high-lying $e_{g\gamma}$ level and to lower lying $e_{g\varepsilon}$ and a_{1g} levels. In the lattice all these levels are broadened into bands. Since the spin-down bands lie below the oxygen 2p(O) bands they do not participate in the optical transition observed in our work; thus, we are concerned with the bands that emerge from the $3d_\beta$ atomic level.

As in Fe_3O_4 above T_V, the number of carriers is half the number of the octahedral sites and the electrons "belong" to these sites, the a_{1g} band will be half-filled, and, hence, the Fermi level E_F will be in the middle of this band. The band structure described above with the proper energy separation between the bands is shown in Figure 2-8. In view of the success of the above approach to interpret the optical results it appears that similar band structure (but not a similar Fermi level) should be observed in α-Fe_2O_3 and FeO.

A very significant and unexpected (based on standard band theory) result in the optical spectra was shown in Figure 2-5. The optical transmission does not vary between 77 and 300 K in spite of the presence of a metal-to-insulator transition at $T_V \approx 120$ K and the jump in activation energy from 0.15 to 0.04 eV at the transition (see Figure 2-1). The result might be interpreted in terms of correlation effects only. This may be discussed in terms of a "Mott-Wigner gap"[7] that, for $T < T_V$, is larger than 0.3 eV; thus, the "Mott-Wigner conduction band" lies within the rather wide $e_{g\varepsilon}$ band. This approach is discussed in detail in Appendix C. The other approach is to assume that the "electron gas crystallization" (see below) does not form a band gap in the sense used in normal band theory. There is very little theoretical work[19-21] on which one can rely in evaluating this assumption. However, the fact that no optical gap is collapsed at T_V explains the so far not understandable transport data. It clearly indicates that for $T < T_V$ the conduction is taking place in the wide $e_{g\varepsilon}$ band and for $T > T_V$ the conduction is in the a_{1g} band (see Appendix C for details).

The metal-to-insulator transition in magnetite has been the subject of experimental and theoretical investigations for more than 40 years. Despite this long period of research, very little understanding has emerged thus far. The difficulty on the experimental side is to get a consistent experimental picture from all the published data. On the theoretical side the fact that correlation effects play a major role did not allow any quantitative approach. In order to gain a better overall picture we have attempted to clarify some of the experimental results that were unclear.

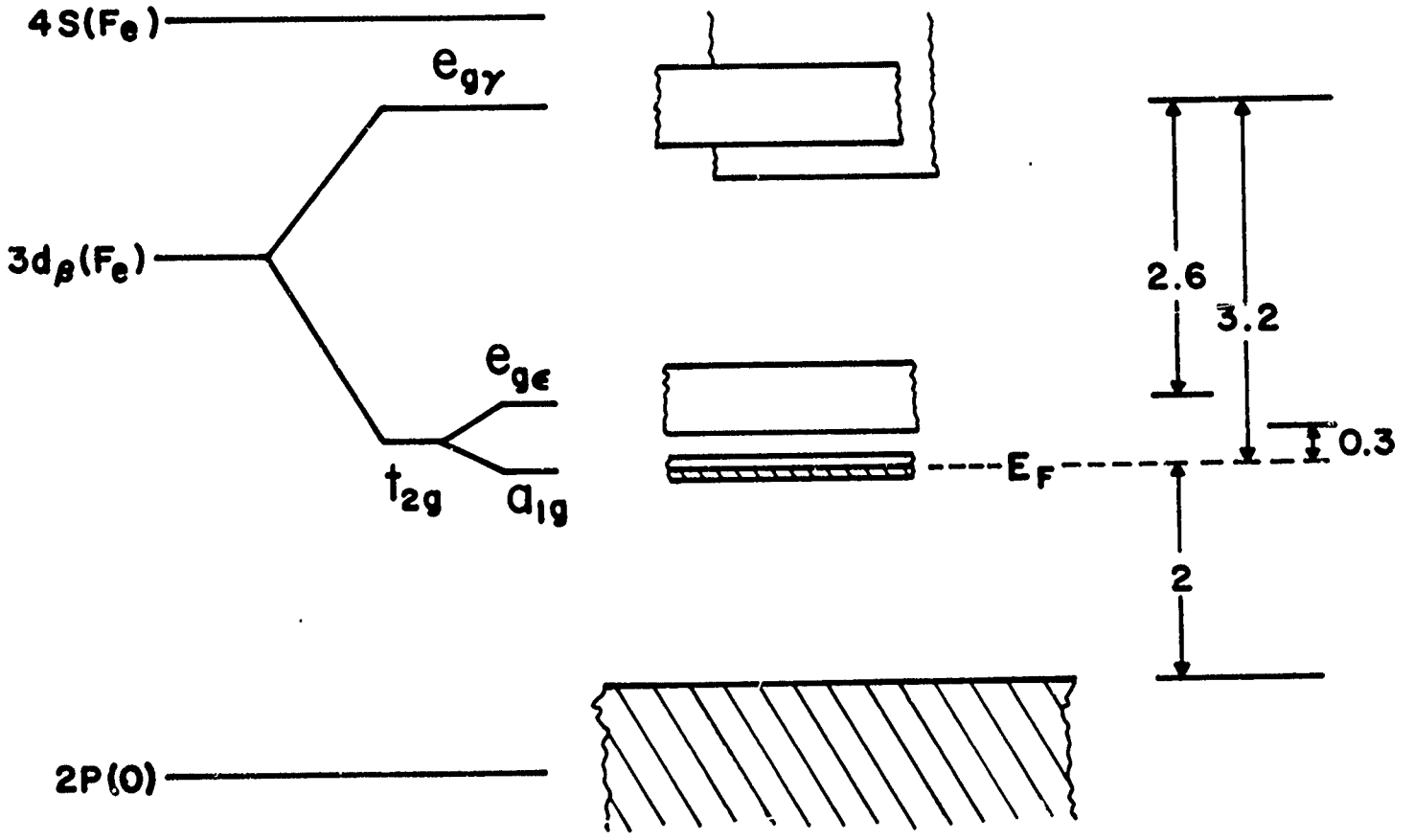

Figure 2-8. Atomic level scheme of an octahedral site in Fe_3O_4, and the proposed energy separations between the corresponding bands in the "metallic" phase.

The effects of nonstoichiometry[11] and doping[12] were unclear in the sense that they do not point out whether these effects are causing the reduction of the transition temperature due to excess carriers (Mott-type transition) or that some exact critical number of carriers is needed so that "crystallization" of the carriers has to take place (Mott-Wigner type transitions). The results that we have described above and those shown in Figure 2-9 indicate that the second possibility is more likely,

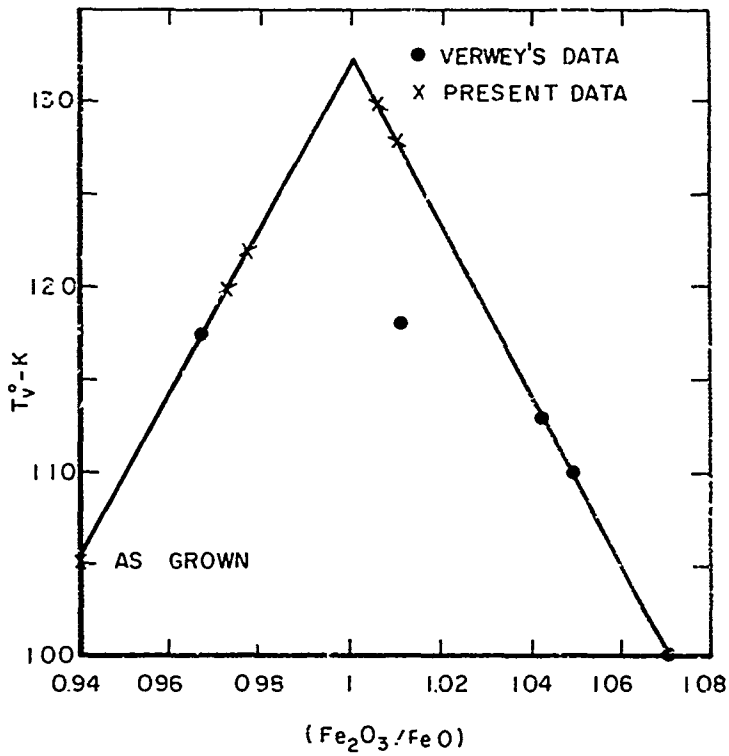

Figure 2-9. The dependence of the transition temperature T_V on the stoichiometry of Fe_3O_4.

and long-range order is established when T drops below T_V. It should be noted that although this was quite expected[7], the Mössbauer data[22] have indicated only localization of carriers. In connection with this problem we have measured the specific heat. Since previous measurements[13] have shown a very smeared peak at T_V, the amount of entropy change at the transition was not clear. The results that we get ($\approx 0.3\ k_B$ per octahedral site) are in accord with the unpublished value quoted by Anderson[14]. However, this number is significantly different from the value he calculated for the Verwey ordering ($\approx 0.2\ k_B$) or the value for a complete order-disorder transition ($k_B \cdot \ln 2$). This and recent Mössbauer[22], N.M.R[22], neutron scattering[23], and electron diffraction[24] experiments all raise serious doubts as to the

applicability of the Verwey ordering scheme. It should be pointed out that this scheme was accepted until two years ago. All this suggests, at least, that the phenomenon of ordering in Fe_3O_4 is more complicated than envisioned by Verwey.

Twenty years ago a more fundamental disagreement with the Verwey scheme was reported by Rooksby and Willis[15]. They found that the distorted low-temperature phase has a rhombohedral symmetry rather than an orthorhombic or tetragonal symmetry as suggested by Verwey. As their experiment was done on powders and was disregarded all these years we wanted to check their results by carrying out the experiment on single crystals derived from various sources. The results have definitely confirmed their claim. It thus seems that a fundamental inconsistency between the Verwey scheme of orthogonal-geometry[11,25] and the crystallographic distortion is obtained. The situation is further complicated by two other results reported in the literature that support orthogonal geometry. These are the observation of a unique [100] axis[26] and the possibility to establish one of the three [100] directions as the magnetic easy axis by cooling magnetite in a magnetic field through the transition[27,28].

In view of all the above we conclude that, before an answer can be found for the mechanism of the insulator-to-metal transition, it will be necessary first to account for the rhombohedral crystallographic symmetry and the uniqueness of the [100] direction. Below are listed a few possible ways to do this, none of which can be clearly ruled out at present.

(1) If one assumes that the rhombohedral symmetry is not connected with the ordering at all, these two contradictory effects can be accounted for. This has some support from the fact that other ferrites go through a crystallographic transition[29,30] around 90 K without any ordering phenomena. One must, however, find a physical explanation for the crystallographic distortion along the [111] axis.

(2) One can assume that the true symmetry is lower than rhombohedral and has a unique [100] axis (say a triclinic symmetry), but only the rhombohedral distortion is large enough to be observed through the transition. One can even find an ordering scheme that will account for this low symmetry. However, from energy minimum considerations, it is not clear why such an ordering will take place.

(3) It might be that the transition takes place in two stages. At the first stage only half of the electrons get localized; this is consistent with rhombohedral symmetry[14]. At the second stage the rest of the electrons get localized but since the first stage ordering is of lower electrostatic energy no appreciable effect on the symmetry is observed. There is no experimental evidence to support this possibility although some people claim to have found a multiple transition[31].

(4) If we assume that the Verwey order is correct in principle, one has to find an interaction that will explain the elongation along one of the [111] axes in the unit cell. Since the magnetic easy axis is the [100] axis it is hard to attribute the rhombohedral distortion to a magnetic interaction. The only interaction that might take place along this axis is the correlation interaction. It is known that the a_{1g} orbitals are oriented along the [111] direction. As the localization takes place the a_{1g} lobes become negatively charged, thus inducing "electrostatic repulsion" between the Fe^{+2} ions that are located along the [111] axes. The advantage with this explanation is that it provides elongation along the [111] axis due to Verwey ordering.

There are difficulties with all the suggestions mentioned above but in view of the importance of correlation effects in this material we believe that the last suggestion is closer to the true explanation than the other three. More studies are needed to resolve the above problem, and only upon its solution can an understanding of the metal-to-insulator transition be hoped for.

III. VANADIUM DIOXIDE

Vanadium dioxide (VO_2) has a rutile structure above $T_V = 68^{\circ}C$ and a monoclinic structure below this temperature. At the transition a change of five orders of magnitude in the electrical conductivity is observed in high-quality crystals. Much experimental work was carried out on this material, and the gross features of its electronic structure are understood[6]. However, only qualitative and unsatisfactory explanations of the transition were given so far. From an application's point of view this is the most promising material since the material's transition temperature can be changed between -150 and 150°C by proper doping, without affecting the abrupt and large change in the conductivity at T_V. The main purpose of this study was to prepare materials suitable for application (films) and to study the metal-to-insulator transition by critical experiments 32 such as the Raman scattering.

A. CRYSTAL GROWTH OF VO_2

Single crystals with dimensions of about 4 x 2 x 0.5 mm^3 were grown by modifying the flux technique reported by Aramaki and Ray[33] . A platinum crucible was filled with V_2O_5 and placed in a high-temperature resistance furnace. The furnace was heated to about 1000°C and maintained at this temperature for times ranging from 24 to 48 hours. During this time, carbon dioxide was passed over the molten V_2O_5. The reducing potential of CO_2 is sufficient to slowly convert the molten V_2O_5 to VO_2 which grows in the V_2O_5 as small single crystals. After the planned growing period has elapsed the mixture is rapidly cooled to 500°C (to terminate further growth), then slowly cooled to room temperature. The remaining V_2O_5 was dissolved in a dilute solution of Na_2CO_3 heated to 70°C.

To dope the VO_2 with Cr we added CrO_2 to the charge. The crystals obtained were comparable in size and quality with the "pure" VO_2 crystals.

B. SPUTTERING OF VO_2 FILMS

VO_2 films were prepared by reactive sputtering at a frequency of 13 MHz. A magnetic field of 50 gauss was used to confine the plasma. The vanadium target had a 6-in. diameter and a 99.999 specified purity. The sputtering gas consisted of argon and 1% oxygen, and the pressure was 25 μmHg. For the present sputtering the separation between the target and the substrate was 2.1 in., and the target voltage was ~820 V. The substrates were glass, oriented sapphire, and oriented rutile, each maintained at 500°C during the sputtering by a radiant heater. The sputtering rate was 10 Å/min.

To get a $(VO_2)_x(TiO_2)_{1-x}$ mixed alloy we replaced the single target by two half discs of vanadium and titanium targets. The substrate for

this study was a 5 in. x 11/16 in. sapphire slide. After the film was made, one end of the slide was VO_2-rich and the other TiO_2-rich. All the other sputtering conditions were those described above. The composition was determined by the method given by Hanak [34].

For electrical measurements In contacts (2000 Å thick) were evaporated on the films. X-ray diffraction has shown that the films are highly oriented and polycrystalline. This method was effective for films thicker than 1000 Å. For thinner films electron diffraction (in reflection configurations) was used. The results of this method had indicated that the crystallites were very small ($\sim$ <100 Å) and on the border of amorphisity.

C. ELECTRICAL CONDUCTIVITY MEASUREMENTS

Four-probe conductivity measurements were carried out on crystals and sputtered films of VO_2 in the temperature range $77 \leq T \leq 370^{\circ}K$. Typical results of the conductivity in the single crystals around the transition region are shown in Figure 2-10. X-ray measurements have shown

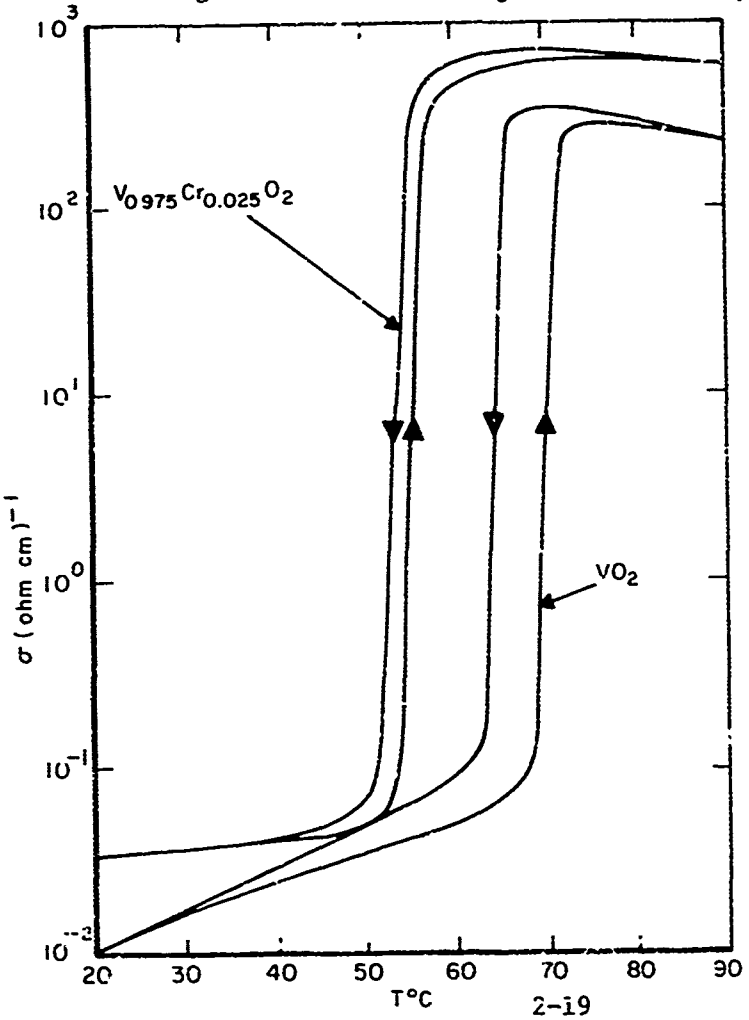

Figure 2-10. Temperature dependence of the conductivity as obtained on single crystals.

that for both the "pure" and the Cr-doped VO_2 the high-temperature phase has a rutile structure. The low-temperature phases were, however, different. For "pure" VO_2 it was monoclinic and for the Cr-doped VO_2 it was orthorhombic. These results are in accord with those of Villeneuve et al.[35]. Recently, Marezio et al.[36] claim that this phase also has a monoclinic symmetry. Significantly, in our Cr-doped VO_2 the transition takes place in a temperature lower than T_V of "pure" VO_2, in contrast with the above-quoted results. It appears that the crystal growth conditions are of importance in determining the crystallographic phase as well as the transition temperature. It is clear that as long as the exact ionization state of the Cr ions in the various crystals is not identified little can be said on the effect of doping on the transition mechanism. It seems that Cr^{+3} ions will cause the transition temperature to drop while Cr^{+5} will cause it to rise. This is probably the reason why Ti-doped VO_2 [37-39] has always a transition temperature lower than that of "pure" VO_2. The effect of high ionicity is both in reducing the number of carriers in the V-Cr-V or V-Ti-V bands and in reducing the extension and thus the overlap of the a_{1g}-wave functions along these vanadium atom "chains".

In view of the above it was expected that if cosputtering of VO_2 and TiO_2 will yield alloys of the type $V_xTi_{(1-x)}O_2$, the transition temperature, at least for the low Ti concentrations, will cause a decrease of T_V with Ti concentration. The conductivity measurements on these systems have shown the reverse behavior as can be seen in Figure 2-11. The other effect as is clearly seen is to broaden the transition region. Since the transition in films is always at temperatures higher than for crystals and both the width and the hysteresis are wider, it appears that a "mechanical" rather than "chemical" effect is observed. The most likely explanation is that the VO_2 and TiO_2 phases coexist, and the TiO_2 phase inhibits the distortion of the VO_2 phase. Since the TiO_2 and VO_2 are not oriented in the present case, the TiO_2 has an effect of "hydrostatic pressure" that is known to cause an increase in T_V. This interpretation has led to the conclusion that holographic storage can be fixed in VO_2 films [40](see below).

The above "mechanical" effect suggests that the equivalent of uniaxial pressure measurements can be achieved by epitaxially growing VO_2 films on proper substrates. Correspondingly, we have compared the effect of sputtering on glass and sapphire with that of oriented rutile. In Figure 2-12 the effect of substrate orientation of the rutile substrate on the transition is clearly demonstrated. Sputtering on the a-a rutile plane (perpendicular to the tetragonal c-axis) causes a decrease in the transition temperature while sputtering on the a-c plane causes an increase in the transition temperature. For thin film the "metallic" rutile structure is kept by the substrate, and the conductivity is much higher than that of the thick films. These results are in accord with the uniaxial pressure measurements of Ladd and Paul[17,41], as will be explained below. In view of the difficulties in producing uniaxial pressures on VO_2 crystals [41] these results seem to provide a new tool for such studies.

D. TUNNELING INTO VO_2 FILMS

The tunneling characteristics of M-I-S (Metal-Insulator-Semiconductor) structures have been used extensively in the past to investigate the electronic structure of semiconductors. One would expect that the collapse of the energy gap of VO_2 at the metal-to-insulator phase transition would manifest itself in a large abrupt change in the I-V characteristics of the M-I-S structure in which the VO_2 is the semiconductor. We have searched for such an effect using a Pt-VO_2-Al_2O_3-In sandwich.

The tunnel junctions were prepared by first sputtering a 1000-Å-thick Pt film on a sapphire substrate. On that film a 1000-Å-thick VO_2 film was reactively sputtered in the manner described above. On top of the VO_2 we have reactively sputtered a 20- to 30-Å film of Al_2O_3. The metal side of the junction was completed by evaporation of In on the Al_2O_3 film. The junctions were first checked without the VO_2, and the measured tunneling characteristics at 1.25 K yielded the proper superconducting energy gap of indium film.

The tunneling characteristics of a VO_2 junction were measured at temperatures between 4.2 and 370 K. The characteristics were strongly nonlinear and did not show much change between 4.2 K and room temperature. Through the transition region the slope of the I-V characteristics for all voltages has indicated a decrease of the tunneling resistance by a factor of three. The slope and the temperature dependence were similar to those observed in M-I-S structures were -S- was amorphous germanium[42]. It thus appears that the first monolayers of the VO_2 films were amorphous and that the main contribution to the tunneling current comes from these layers. Indeed, photoemission studies[43] from VO_2 indicate that a 10- to 20-Å layer on crystalline VO_2 is amorphous. The entire film was not amorphous. This was found from the three-orders-of-magnitude jump in the conductivity of the material (measured in a planar geometry), while it is known that the transition is not found[44] in amorphous VO_2.

E. APPLICATION OF VO_2 FILMS

The high quality of the films and the feasibility of using them for practical application was demonstrated by two separate studies[40, 45] connected with the present VO_2 research program.

The first study was concerned with a permanent-erasable holographic storage on VO_2 films by utilizing the change in the optical properties of the material when it passes through the transition. The possibility to have this application relies on the coexistence of both phases at a single temperature due to the "mechanical" strains in the films (see above). The "writing" was done by laser pulses as we have described previously[1,2] (for details see Ref. 40).

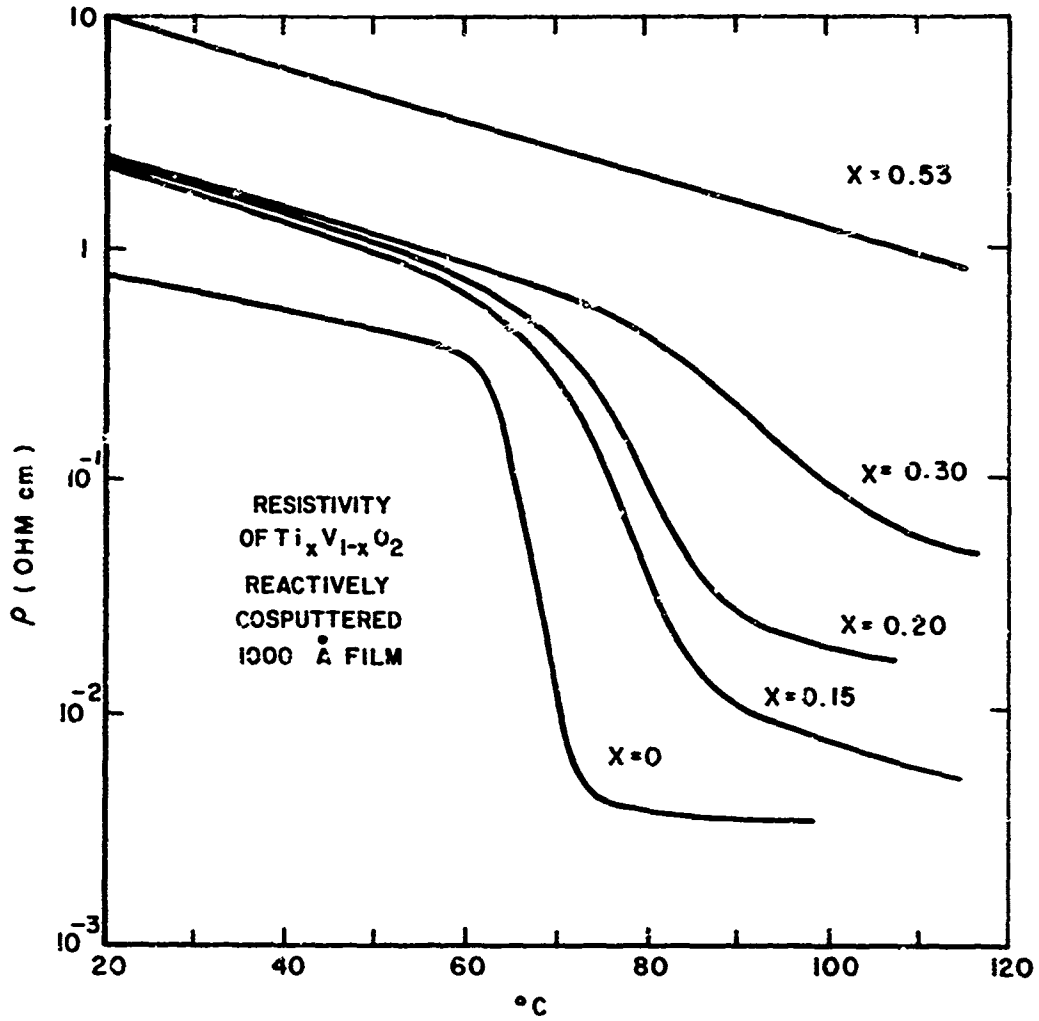

Figure 2-11. Temperature dependence of the resistivity $(TiO_2)_x(VO_2)_{1-x}$ co-sputtered films.

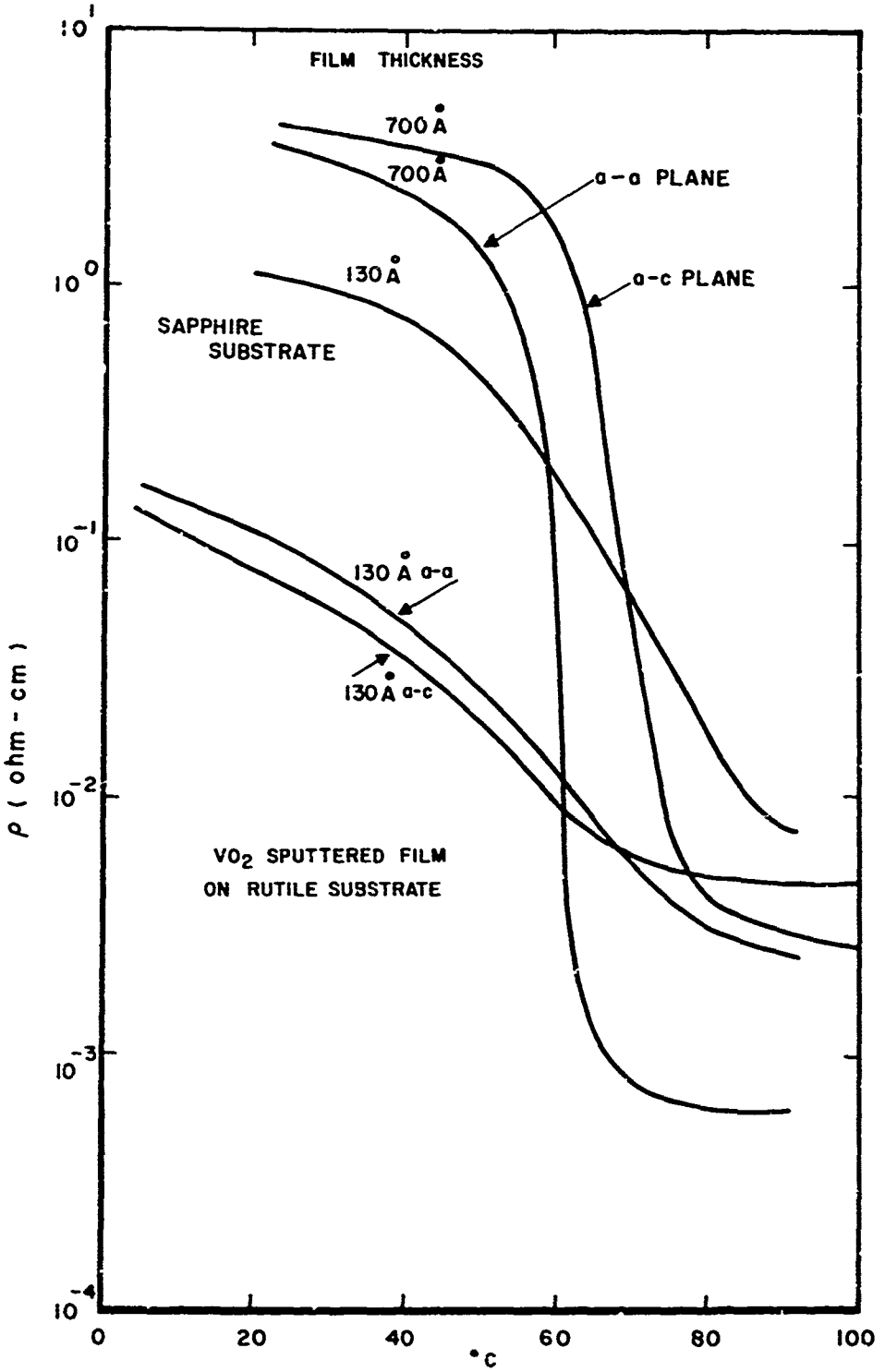

Figure 2-12. Temperature dependence of the resistivity as obtained on sputtered VO_2 films.

The other application was the use of VO_2 films as an electron beam recording medium[45]. A comparison of a theoretical analysis of the transient temperature profile (produced by an electron beam scanning a planar structure as applied to VO_2 on mica) with the experiments, has shown that: (1) there is little diffusion of heat in the VO_2 film; (2) the minimum size of transformed region must be >1000 Å, and (3) VO_2 is comparable in sensitivity to photoresist as an electron beam recording material (for details see Ref. 45).

F. RAMAN SCATTERING STUDIES

In our hope to gain some understanding on the mechanism [1,2,17] for the metal-to-insulator transition in VO_2 we constructed a sensitive Raman scattering experiment with a back-scattering geometry (since VO_2 is opaque to light available from proper laser sources). The main components of the system were a Spectra Physics 165 krypton ion laser, a Spex 14000/II spectrometer, an Intertechnique-Didoc 800 multichannel analyzer, an EG&G -M-100 modular counting system, and an RCA C-31034 photomultiplier.

Typical results of the spectrum obtained are shown in Figure 2-13. These results were obtained at room temperature on VO_2 powders, hot-pressed powders, and single crystals. They are quite different from the results reported by Chase and Srivastava [46]. Careful examination of the results made us suspicious that the spectra observed are those of V_2O_5 that might be formed on the VO_2 surface due to the heating by the laser beam. Correspondingly, we have grown V_2O_5 crystals. Running the spectra of V_2O_5 has produced the spectra shown in Figure 2-14. The spectra are identical.

To eliminate the oxidation we have mounted the VO_2 crystals in an evacuated cold-finger dewar that was kept at 77 K. No spectra were observed then. We thus suspect that the crystals of Chase and Srivastava were different from ours[46,48]. They kindly supplied one of their crystals but we could not obtain any spectra on their sample either.

With confidence in our system and knowing that other groups[47] have observed the same spectra that we have and in view of the inconsistencies in the reports of Chase and Srivastava[46,48,49], we were left with very little confidence in their results. It appears that the VO_2 spectra, cannot be observed by conventional Raman spectroscopy.

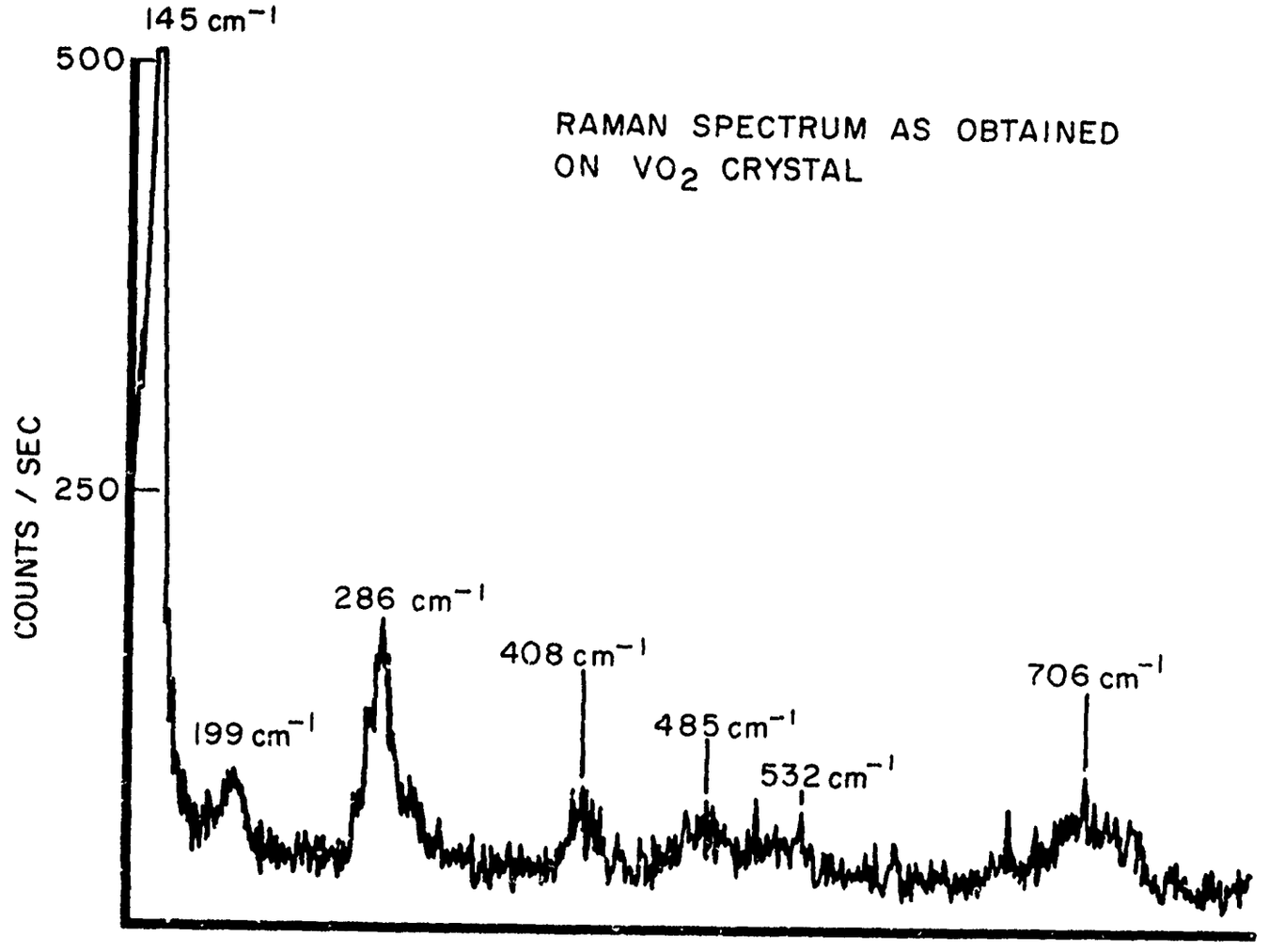

Figure 2-13. Raman spectrum as obtained on VO_2 crystal at 300 K with a laser power of 300 mW.

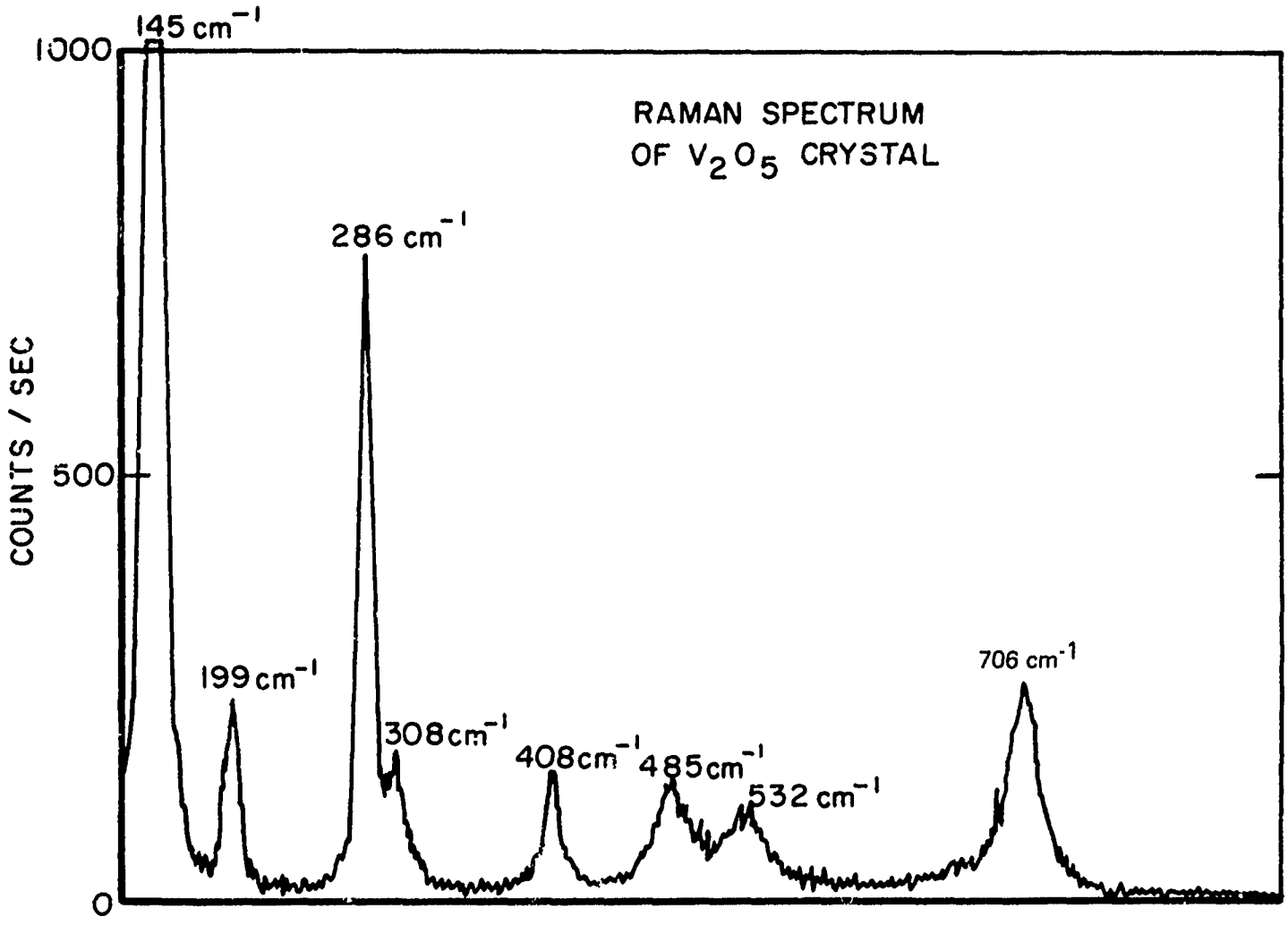

Figure 2-14. Raman spectrum of V_2O_5 at 300 K.

G. SUMMARY AND CONCLUSIONS

In the work described above we have demonstrated the possibility of producing VO_2 crystals and films where the transition temperature and the transition sharpness can be affected by proper preparation. We have found that it is necessary for the lattice to distort in order to have the conductivity transition. We have further shown that the effects of pressure on the transition can be studied by sputtering techniques.

VO_2 crystals are very fragile and they crumble when they are cycled through the transition. This is not the case with VO_2 films. However, unlike V_2O_3 films the present films can have a conductivity jump of four orders of magnitude at the transition and can be cycled through the transition indefinitely. There is a slight increase in the unit cell volume when warmed through the transition; therefore, hydrostatic pressure causes an increase[50] in T_V. Since the effect of TiO_2 doping would clearly be to lower the transition temperature[38,39], the observed increase of T_V with x in the $(TiO_2)_x(VO_2)_{1-x}$ mixture is due to inhibition of the VO_2 lattice distortion by the TiO_2 phase. The measured hydrostatic effect is $dT_V/dp = 6.10^{-2}$K/kbar. In our case $dT_V/dx \approx 0.6$ K/(1% TiO_2) for up to x = 0.4. Correspondingly, for the present conditions $dp/dx \approx 10$ kbar/(1%TiO_2).

The effect of uniaxial pressure was reported previously[17,41] to just broaden the transition, in the case of single crystals, when it was applied along the a-axis. When the pressure was applied along the c-axis, it did not broaden the transition but decreased T_V. The maximum pressure achieved on crystals before breaking them was 0.5 kbar, and it was found [17] that $(dT_V/dp_c) = 1.2$ 10 K/kbar. The effect of the substrate in our case is similar except that it causes negative pressure rather than a positive one. This can be seen from Table I where the lattice constant of the high-temperature phase of VO_2 (VO_2-rutile) is compared with that of monoclinic VO_2 and TiO_2. For the monoclinic VO_2 we have used the pseudo-rutile axes that emerge from the high-temperature phase rutile axes.

TABLE I

LATTICE CONSTANTS OF VO_2 and TiO_2

	VO_2 (Rutile)	VO_2 (monoclinic)	TiO_2
a(A^o)	[illegible]530	5.375	4.593
b(A^o)	[illegible]	4.517	4.593
c(A^o)	[illegible]59	2.871	2.959

The effect of uniaxial pressure[17] along the a-axis is to aid the contraction of the pseudo b-axis but to inhibit the elongation of the pseudo a-axis. Since the material at the transition is splitting into pseudo a- and pseudo b-domains the effect might be only to broaden the transition. The effect of the TiO_2 a-a plane on the epitaxially grown film is opposite to that of the pressure; it inhibits the contraction of the pseudo b-axis thus causing a decrease in T_V. Along the c-axis we see that: C(TiO_2)>C(monoclinic VO_2)>C(rutile VO_2); thus, the substrate is expected to have the effect of negative pressure, i.e., to increase the transition temperature.

These results show that changes along the c-axis, though small, are very critical. This indicates that indeed it is the V-V separation that is the most important variable in the transition mechanism[51].

The failure of the attempt to get a VO_2 Raman spectra, the doubts as to the previous reported spectra and the inconclusiveness of these reported results are very disappointing. They indicate that either another critical experiment has to be designed[2] or no progress will be achieved until quantitative theoretical work on the band structure and phonon spectra of VO_2 is done. From the application point of view we have demonstrated the versatility and wide spectra of application of this special material.

IV. POLARON SWITCHING

Two years ago Hed and Freud[5] proposed a switching mechanism based on the assumption that in a high electric field one can change the effective electron-phonon interactions and thus bring about a dis-association of polarons at some critical electric field. This critical field depends on a "microscopic"[5] dielectric constant that was not calculated in their work. In the experimental part of their work two oxides were used, $Co_{(1+y)}Cr_{2-y}O_4$ and $Co_{(1-x)}Li_{(x)}O$ (where x = 0.06). These materials have exhibited a switching effect. In their work no single attempt was made to correlate the experiment with theory. Closer examination shows in fact that experiment and theory disagree since the critical field for $Co_{(1-x)}Li_xO$ switching was $(200/5.10^{-3}=)$ 4.10^4V cm while the value computed from their theory should be much higher. In their paper no comment was made about this discrepancy nor did they mention the doubts [52] as to the existence of polarons in the transition metal monoxides.

Although both their theoretical analysis and experimental work are questionable, we have approached the basic idea of their paper theoretically and experimentally. For experimental tests we have used the only material (TiO_2) in which little doubt exists as to the polaronic nature of the charge carriers[53,54] .

A. THEORETICAL EXAMINATION OF "POLARON SWITCHING"

We first sketch the Hed and Freud[5] model. We then comment on their numerical estimates and on the physical validity of their model.

The model is based on Holstein's, Molecular-Crystal-Model (MCM) of small polaron motion[55]. This assumes a linear chain of diatomic molecules, each with fixed orientation and center gravity, but with variable internuclear separation, u_n. The potential energy of the n^{th} neutral diatomic molecule is, neglecting vibrational coupling between adjacent molecules, simply

$$\frac{1}{2} M \omega_o^2 u_n^2 \qquad (1)$$

where M is the reduced mass of the diatomic model and ω_o is its natural frequency of vibration (Einstein approximation). The interaction between the displacement u_n of the occupied molecule and the excess (electron or hole) charge carrier is taken to be linear in the local displacement coordinate (as is standard in nearly all treatments of the electron-phonon interaction):

$$- A u_n \qquad (2)$$

The sum of Eqs. (1) and (2) describes a mono-negative-molecule ion

(for an excess electron) with a new equilibrium position

$$u_n^{\,o} = A/M\omega_o^{\,2} \tag{3}$$

and bound with a binding energy

$$E_b = -A^2/2M\omega_o^{\,2} \tag{4}$$

In an externally applied electric field, Hed and Freud's procedure is to augment the energy with the term

$$e\,F\,\&(n)\,u_n \tag{5}$$

where F is the electric field strength, and $\&(n)$ is a "microscopic dielectric constant" that is discussed later.

Hed and Freud state that the addition of Eqs. (5) and (2) represents an "effective reduction" of the electron-phonon interaction as given by an effective interaction constant

$$A_{eff} = A - e\,F\,\&(n) \tag{6}$$

Now, a site jump transition from the initially occupied molecule ion n to a neighboring ion (n + 1) occurs at a coincidence (c) of the electronic energies

$$A\,u_n^{\,c} = A\,u_{n+1}^{\,c}$$

The lowest energy configuration corresponding to this is due to a thermal fluctuation which removes one half of the distortion on site n and produces one half of the distortion on site (n + 1); i.e.,

$$u_n^{\,c} = u_{nH}^{\,c} = \frac{1}{2}\,u_n^{\,o} \tag{7}$$

where $u_n^{\,o}$ is given by Eq. (3).

The activation energy $E_a = \frac{1}{2}\,|E_b| = \frac{A^2}{4M_o^{\,2}}$

Freud and Hed's procedure is to replace A by A_{eff}, so that

$$E_a\,(F) = \frac{A^2_{eff}}{4M\omega_o^{\,2}} = \frac{1}{4M\omega_o^{\,2}}\left[A - e\,F\,\&(n)\right]^2$$

Now the condition for localization and small polaron formation is simply that the binding energy gained by localization exceed the banding energy which can be gained by delocalization in a rigid lattice, viz.

$$\frac{A^2}{2M\omega_o^2} > 2J$$

Freud and Hed assume that, in the presence of an electric field, this is changed to

$$\frac{A^2_{eff}}{2\,M\omega_o^2} > 2J \qquad (8)$$

They claim that delocalization will occur at that electric field F_b which produces a reduction of A_{eff} [Eq.(6)] so as to give an equality in Eq.(8).

$$F_b = \frac{A - (4\,J\,M\omega_o^2)^{1/2}}{\epsilon\,(n)} \qquad (9)$$

Taking $M \cong 3.6 \times 10^{-26}$ kg, $\omega_o \cong 10^{13}$ sec^{-1}, $A \cong 4.8 \times 10^{-10}$ joule meter^{-1}, $J = 0.05$ eV, $\epsilon\,(n) = 10$, they obtain $F_b' = 1 \times 10^6$ V cm^{-1}; if $\epsilon\,(n) = 100$, they obtain $F_b = 1 \times 10^5$ V cm^{-1}.

Comments

I. If we accept their model, we see that the choice of constants corresponds to a zero (zero field) polaron binding energy [Eq.(4)]

$$E_b = \frac{A^2}{2M\omega_o^2} = \frac{(4.8 \times 10^{-10})^2}{2 \times 3.6 \times 10^{-26} \times 10^{26}} \cong 3.2 \times 10^{-20} \text{ joules} \cong 0.2 \text{ eV} \qquad (10)$$

which is of a reasonable magnitude.

II. Their reason for the introduction of a "microscopic dielectric constant" in Eq.(5) is that the time over which the jump occurs, $[\hbar/A(kT/M)^{1/2}]^{1/2}$, is much less than the stay time at a given site (~reciprocal of the jump rate); therefore, the electric field acts only over the displacements and not between the sites.

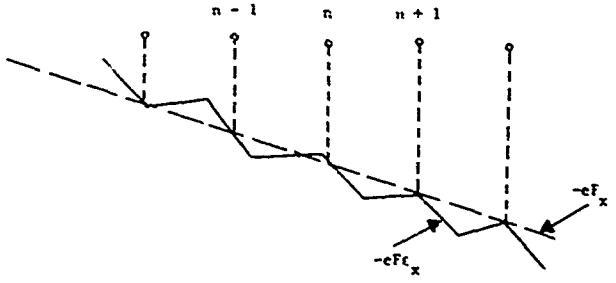

But there is no physical basis for such an assumption. The effective field cannot be very different from the applied field. In particular, it is seen from Eq.(9) that if ϵ (n) is taken to be 1 instead of 10 to 100, the breakdown fields F_b become 10^7 V/cm.

III. An even more basic criticism is that the local field energy [Eq.(5)] is inappropriate because the displacements u_n represent the deviation from equilibrium of the internuclear spacing of a diatomic molecule, *not* the absolute displacement of an electron in a constant electric field. In fact, their effective interaction constant [Eq.(6)] depends linearly on F (both in magnitude and sign), so that A_{eff} is *increased* if the direction of F is reversed. Clearly this is unphysical.

Even if one had an atomic lattice, rather than a molecular-crystal-model, the relation (5) would not be valid. In this case, u_n represents the displacement from equilibrium of the n^{th} atom. But since the electron would tend to follow the motion of its atom relation, (5) should not apply; rather, the electric field can affect only the *internal* energy and structure of the atom + electron system.

To see how the electric field does enter, we note that the wave equation for one excess electron in the crystal is

$$[H_o + e \underset{\sim}{F} \cdot \underset{\sim}{r}] \Psi = E \Psi \tag{11}$$

where H_o is the field free Hamiltonian. Now $\Psi(r)$ is represented as a superposition of local atomic (or Wannier) states with coefficients a_n which depend on all the displacements (... u_n ...):

$$\Psi = \sum_n a_n \varphi_n(\underset{\sim}{r} - \underset{\sim}{n}; u_n) \tag{12}$$

The wave equation of the n^{th} site is

$$[H_n + e\underset{\sim}{F} \cdot (\underset{\sim}{r} - \underset{\sim}{n})] \varphi_n(\underset{\sim}{r} - \underset{\sim}{n}; u_n) = \varphi_n (\underset{\sim}{r} - \underset{\sim}{n}; u_n) \tag{13}$$

The procedure is to substitute Eq.(12) into Eq.(11) and make use of Eq.(13) to obtain an equation of motion for the site occupation probabilities, a_n. In so doing, the electric field term in Eq.(11) is simply decomposed into

$$e \underset{\sim}{F} \cdot \underset{\sim}{r} = e \underset{\sim}{F} \cdot \underset{\sim}{n} + e \underset{\sim}{F} \cdot (\underset{\sim}{r} - \underset{\sim}{n})$$

where the second term is the *local* electric field energy appearing in Eq.(13), leaving the first term in the equation for the a_n:

$$[H + e \underset{\sim}{F} \cdot \underset{\sim}{n}] \quad a_n = E \, a_n \tag{14}$$

In summary then, the electric field appears in two ways. First, it modifies the energy and wave function of each localized state according to Eq.(13), and, secondly, it superimposes an energy gradient on the net motion according to Eq.(14).

According to the second mechanism [Eq.(14)], the electric field will have an appreciable effect in delocalizing the polaron when the intersite electric field energy eFa becomes comparable with the binding energy which was estimated in Eq.(10). Thus, $eF_b a \gtrsim 0.2$ eV requires that $F_b \gtrsim 10^7$ V cm^{-1} for a = 3 Å.

According to the first mechanism, contained in Eq.(13), there can be an electric-field induced modification of the local states, φ_n. If such an effect increases J (rather than decreasing A_{eff}), Eq.(8) could be turned into an equality, in principle. However, a nondegenerate state, usually assumed in the treatment, has no first-order Stark effect. The effect would be at least second order in the parameter

$$\left(\frac{\text{electric field energy over Bohr radius}}{\text{unperturbed electronic energy differences}} \right),$$

and would therefore be small. Possibly, some highly polarizable, non-isotropic, atomic or molecular state might be found for which there is a large electric field enhancement of J.

B. HIGH FIELD EFFECTS IN TiO_2

In order to test the polaron switching we were looking for switching effects in TiO_2. This material, when pure, has a dielectric strength of the order of 10^5 - 10^6 V/cm[56-60]. To test the material in this range, that is the expected range for "polaron switching", we have used thin films and thin single crystals.

The films were made by first sputtering Pt on a TiO_2 substrate in order to make the TiO_2 film to grow epitaxially. On the Pt, we have sputtered reactively the TiO_2 film under the same condition mentioned above for VO_2. On top of this 1000-Å TiO_2 film gold contacts were evaporated. Electron microscopy has shown that the films were polycrystalline with crystallite size $\gtrsim$100 Å, thus bordering on amorphousness. In these films it was impossible to confirm that the charge carriers are indeed polarons because the only acceptable test so far[53] is to compare the absorption coefficient α at λ = 1.5 μm to the conductivity[61]. The ratio α/σ should be of the order of 5.10^2 ohm. Thus, with existing optical techniques this α cannot be measured on such thin films. However, to check the proposed idea we tried to switch the material. We have used short pulse techniques to measure the I-V characteristics and the results are shown in Figure 2-15. Up to a certain critical field ($\sim 2 \cdot 10^6$ V/cm) the material seems to heat up.

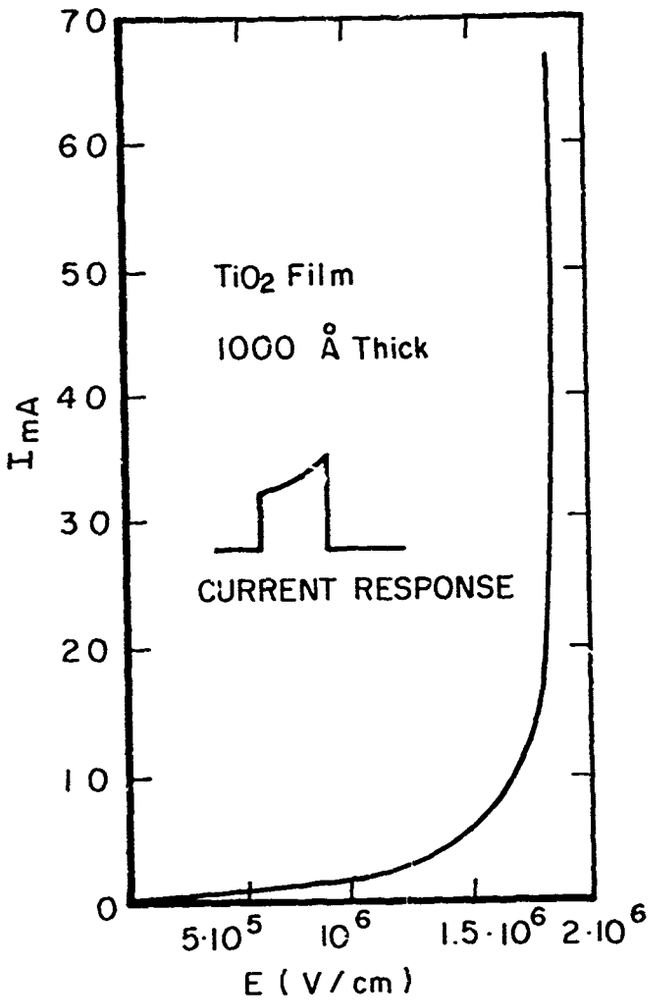

Figure 2-15. I-V characteristics of a sputtered TiO_2 films. Also shown is the shape of the current response to a square voltage pulse, indicating heating effects.

Then a destructive breakdown is observed. No reversible switching effect was observed.

In view of the above we have prepared crystals that definitely "pass the only available test"[61] of polaron existence. This was done by reducing TiO_2 crystals at 800°C in a vacuum of 10^{-2} mm Hg for the proper length of time (that depends on the α desired). The typical optical spectra of the treated samples are shown in Figure 2-16. It is apparent that for this material α/σ ratio is of the right order. We have thinned these crystals to 100 μm and then tried both ac and pulse techniques. Contacts to the samples were made by soldering In to a smeared In-Hg amalgam on the surface. With materials having observable α, heating effects were found to be so strong that a hole was burned through the material at ac fields of the order of 10^3 V/cm. We have thus used pulse techniques with a box car integrator to monitor the I-V characteristics. The results were much the same except that the holes were burned at about 10 10^4 V/cm when the pulse width was about 5 μsec wide. No switching or high field effects predicted by polaron theories[62,63] were found.

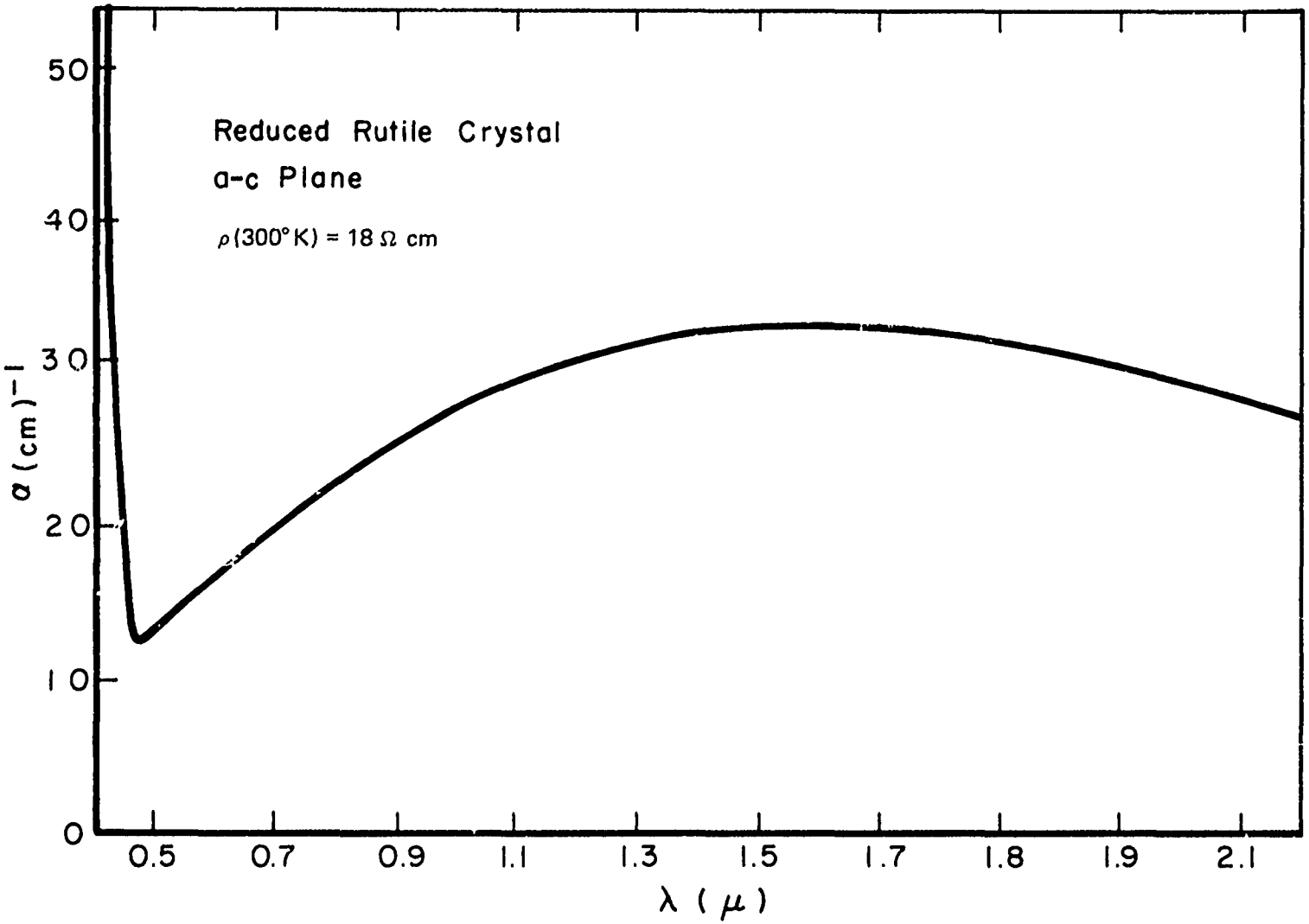

Figure 2-16. The absorption coefficient of the oxygen-reduced TiO_2 crystals that were used for the high electric field measurements.

C. SUMMARY AND CONCLUSIONS

In view of all the above we do not see theoretically a way, by which electric field-induced dissociation of polaron can be achieved with realizable fields of 10^5 - 10^6 V/cm. On the experimental side we see that heating effects in low-mobility materials, polaronic or others, will always occur at fields lower than those required for polaron dissociation. We must thus conclude that at present this mechanism is not amenable to an experimental test. It might be amenable if one can find a new criterion for polaron identification so that both this criterion and proper switching characteristics are found in the same material.

REFERENCES

1. W. R. Roach and I. Balberg, Solid State Commun. 9, 551 (1971).
2. I. Balberg and W. R. Roach, in *Conductivity in Low-Mobility Materials*, p 77, (1971).
3. I. Balberg, Phys. Rev. Letters 25, 1294 (1970).
4. I. Balberg, Appl. Phys. Letters 18, 562 (1971).
5. Z. Hed and P. J. Freud, J. Non-Crystalline Solids 2, 484 (1970).
6. D. Adler, Solid State Physics 21, 1 (1968).
7. N. F. Mott, Phil. Mag. 20, 1 (1970).
8. Z. Hauptman, Czech. J. Phys. B12, 148 (1962).
9. R. Kershaw and A. Wold, Inog. Syn. 11, 10 (1968).
10. I. Balberg and J. I. Pankove, Phys. Rev. Letters 27, 596 (1971).
11. E. J. W. Verwey and P. W. Haayman, Physica 8, 978 (1941).
12. P. A. Miles, W. B. Westhal, and A. Von Hipple, Rev. Mod. Phys. 29, 279 (1957).
13. B. S. Ellepson and N. W. Taylor, J. Chem. Phys. 2, 58 (1934).
14. P. W. Anderson, Phys. Rev. 102, 1008 (1954).
15. P. H. Rooksby and B. T. M. Willis, Acta. Cryst. 6,565 (1953).
16. G. A. Samara, Phys. Rev. Letters 21, 735 (1968).
17. L. Ladd, Ph.D. Dissertation, Harvard University (1971).
18. T. J. Moran and B. Lüthi, Phys. Rev. 187, 710 (1969).
19. W. F. Brinkman and T. M. Rice, Phys. Rev. B2, 1324 (1970).
20. R. A. Bari, D. Adler, and R. V. Lange, Phys. Rev. B2, 2898 (1970).
21. M. Weger, Phil. Mag. 24, 1095 (1971).
22. M. Robinstein and D. W. Forester, Solid State Comm 9, 1675 (1971).
23. E. J. Samualsen, et al., J. Appl. Phys. 39, 114 (1968).
24. T. Yamada, K. Suzuki, and S. Chikazumi, Appl. Phys. Letters 13, 172 (1968).
25. J. R. Cullen and E. Callen, Phys. Rev. Letters 26, 236 (1971).
26. W. C. Hamilton, Phys. Rev. 110, 1050 (1958).
27. B. A. Calhoun, Phys. Rev. 94, 1577 (1954).
28. S. C. Abrahams and B. A. Calhoun, Acta Cryst. 8, 257 (1955).

29. H. P. Rooksby and B. J. M. Willis, Nature 172, 1054 (1953).

30. L. R. Bickford, Phys. Rev. 78, 449 (1950).

31. B. J. Evans and E. F. Westrum, Phys. Rev. B., to be published.

32. W. Paul, Mat. Res. Bull. 5, 691 (1970).

33. S. Aramaki and R. Ray, J. Mater. Sci. 3, 643 (1968).

34. J. J. Hanak et al., J. Mater. Sci. 5, 964 (1970).

35. G. Villeneuve et al., Mat. Res. Bull. 6, 119 (1971).

36. M. Marezio et al., Phys. Rev. B5, 2541 (1972).

37. I. Kristensen, J. Appl. Phys. 39, 5341 (1968).

38. C. N. R. Rao et al., J. Phys. Chem. Solids 32, 1147 (1971).

39. J. M. MacChensney and H. T. Guggenhaeim, J. Phys. Chem. Solids 30, 225 (1969).

40. W. R. Roach, Appl. Phys. Letters 19, 453 (1971).

41. L. Ladd and W. Paul, Solid State Comm. 7, 425 (1969).

42. T. W. Osmun and H. Fritzsche, Appl. Phys. Letters 16, 87 (1970).

43. R. J. Powell, C. N. Berglund, and W. E. Spicer, Phys. Rev. 178, 1410 (1969).

44. T. N. Kannedy and J. D. Mackenzie, J. Non-Crystalline Solids 1, 326 (1969).

45. W. R. Roach, to be published.

46. L. L. Chase and Ramakant Srivastava, Phys. Rev. Letters 27, 727 (1971).

47. P. M. Raccah, private communication.

48. L. L. Chase and Ramakant Srivastava, in *Light Scattering in Solids*, p. 380 (1971).

49. L. L. Chase, private communication.

50. C. N. Berglund and A. Jayaraman, Phys. Rev. 185, 1034 (1969).

51. L. B. Goodenough, J. Solid State Chem. 3, 490 (1971).

52. D. Adler and J. Feinleib, Phys. Rev. B2, 3112 (1970).

53. I. G. Austin and N. F. Mott, Adv. Phys. 18, 41 (1969).

54. H. G. Reik, in *Conductivity in Low-Mobility Materials*, p. 135 (1970).

55. T. Holstein, Ann. Phys. 8, 343 (1959).

56. D. A. Powers and I. J. T. Johnsen, J. Appl. Phys. 32, 1083 (1961).

57. E. H. Greener, D. J. Fitzerald, and W. M. Hirthe, J. Appl. Phys. 37, 443 (1962).

58. G. G. Engelfield, IEEE Trans. Elect. Devices ED-14, 443 (1967).
59. J. Hada, Japanese J. Appl. Phys. 9, 1078 (1970).
60. F. H. Greener and D. H. Whitemore, J. Appl. Phys. 32, 1320 (1960).
61. V. N. Bogomolov et al., Soviet Physics-Solid State 9, 1630 (1968).
62. P. R. Emtage, Phys. Rev. B3, 2685 (1971).
63. A. L. Efros, Soviet Physics-Solid State 9, 901 (1967).

APPENDIX C

VOLUME 27, NUMBER 9 PHYSICAL REVIEW LETTERS 30 AUGUST 1971

Optical Measurements on Magnetite Single Crystals*

I. Balberg and J. I. Pankove
RCA Laboratories, Princeton, New Jersey 08540
(Received 2 June 1971)

Optical transmission and reflectance were measured on natural magnetite single crystals in the spectral range $0.15 \leq h\nu \leq 0.75$ eV. These measurements below and above the semiconductor-to-metal transition temperature T_v have shown that, unlike for the vanadium oxides, there is no collapse of the optical gap at the transition. The present results and the existing data on the transport properties of magnetite indicate that different bands contribute to the electric conduction above and below T_v.

Magnetite, Fe_3O_4, is one of the early materials for which it was realized that the Wilson band theory does not apply,[1] and it is the first material in which a semiconductor-to-metal phase transition was found.[2] This transition takes place at the so-called Verwey temperature, $T_V = 119$°K. While many studies on the electrical and magnetic properties of this material have been made,[3,4] very few and limited optical data are available for this material.[5-7] Only room-temperature reflectivity has been studied so far on single crystals,[5] while optical absorption studies were carried out only on films[6] (for photon energies $h\nu > 1.5$ eV) and powders[7] (for $h\nu \leq 0.2$ eV). Furthermore, no optical constants were determined.

In magnetite the spin-down d bands can be regarded as fully occupied and well separated from spin-up d bands. These spin-up bands are split by the crystal field into two doublets and one low-lying singlet band. This singlet band should be half filled and thus yield metallic behavior.[8] However, for $T < T_V$ magnetite exhibits a semiconducting behavior, and an energy gap due to interatomic correlation energy[9,10] is expected[10,14] to split up this singlet band. We shall call this energy gap, E_{MW}, the Mott-Wigner (MW) energy gap, and the corresponding bands that emerge, the MW valence band and the MW conduction band. As the energy E_{MW} is expected[12,14] to be within the previously unexplored optical range and as the largest measured[3,12,14] conductivity-activation energy in the purest magnetite crystals just below T_V is 0.15 eV, it appears that the spectral range $1.5 \geq h\nu \geq 0.15$ eV should be studied. Furthermore, to understand the nature of the transition it is extremely important to study the optical properties in this spectral range above and below the transition temperature. There is no earlier determination whether an optical energy gap is or is not produced when the material is cooled below the transition temperature, while theoretical models for this material are strongly dependent on the formation of an energy gap.[4,9,12] In V_2O_3 and VO_2, investigations below and above the transition temperature have shown that at the transition, the optical band gap had collapsed.[15-18] As we shall see below, the case of Fe_3O_4 is different and therefore appears to be the first transition-metal oxide that exhibits the semiconductor-to-metal transition while the optical measurements do not indicate any band overlap.

For the present study, we have used natural magnetite single crystals. The lattice constant of the crystals is 8.396 ± 0.001 Å, and their main impurities are Ti (≈ 1.0 wt%) and Zn (0.15 wt%) while the total content of the other metallic impurities was about 0.1%. The crystals were cut into slices, the planes of which were perpendicular to the crystallographic [111] direction. These slices were polished down to 50 or 25 μm and cemented to a CaF_2 wafer.

In Fig. 1 we show the typical temperature dependence of the conductivity of the actual samples used for the optical measurements. This dependence is similar to that observed in the many earlier studies.[3,4,19] The activation energy increases from 0.05 eV at very low temperature to about 0.1 eV just below the transition and is 0.04 eV just above the transition. This 0.04-eV value seems to be independent of sample purity.[9,19,20]

For the optical measurements, the sample was placed on an apperture. Transmission measurements were made by the sample-in, sample-out technique in which the sample-out condition consisted of replacing the mounted specimen by an identical CaF_2 wafer without magnetite.[14]

The optical relative transmission I/I_0, the reflectance R, and the absorption constant α are related by

$$I/I_0 = (1 - S)(1 - R)^2 \exp(-\alpha d), \quad (1)$$

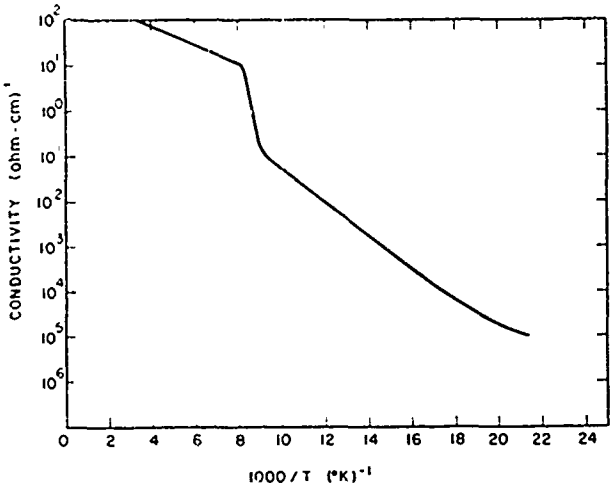

FIG. C-1. The conductivity dependence on temperature of crystals used for the optical measurements.

where S is the fraction of light scattered and d is the thickness of the sample. In Fig. 2 we show the results of the measurements of I_0/I and R as functions of the incident photon energy for a 25-μm-thick sample and the α deduced from these results using Eq. (1). The results shown in Fig. 2(a) indicate that the absorption edge starts at about *0.3 eV* and rises slowly to higher energies. The actual absorption edge is expected to rise faster than shown in Fig. 2(a) as can be seen if one subtracts the contribution of those absorption processes which cause the absorption to increase with decreasing photon energy and which are dominant below 0.3 eV. As for V_2O_3,[15,16] the broad absorption edge is probably due to band tails that are expected to be formed by imperfections and strong correlation effects.[21] Two sharp absorption peaks are observed at 0.16 and 0.21 eV; their origin is not understood, but it is conceivable that these peaks may be associated with the Ti and Zn impurities. The most striking and important result is the fact that only very *minor* changes in the absorption spectrum are observed while passing through the transition temperature, in significant contrast to the behavior of the vanadium oxides. This fact will be discussed below. No significant difference was observed between different samples.

Because of the strong absorption above $h\nu = 0.75$ eV, we were unable to measure the transmission above this energy in single-crystal samples. Using an Fe_3O_4 film we have extended the transmis-

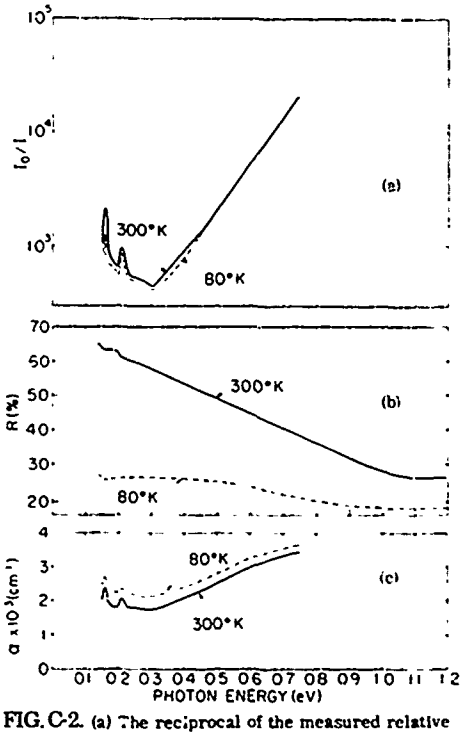

FIG. C-2. (a) The reciprocal of the measured relative transmission and (b) the reflectivity of a 25-μm-thick, natural magnetite crystal. (c) The absolute absorption coefficient, obtained from (a) and (b).

sion measurements to the 0.5 $h\nu$ < 4 eV range.[11] Again no significant change was found by cooling the sample from 300 to 80 K. The film absorption was similar[11] to that reported by Miles, Westphal, and von Hippel.[7]

In Fig. 2(b) we show the magnetite reflectance versus incident photon energy, as compared with that of evaporated Al, for 300 and 80 K. Our results are in good agreement with the earlier measurements of the reflectance spectra of ferrites at room temperature and with the dependence of the reflectance in these materials on their conductivity. The reflectance dependence on the wavelength, and the agreement with the results obtained with ferrites, indicate that the main contribution to the 300°K reflectance is due to "free" carrier absorption while at 80 K the main contribution is due to interband transition. We put the word free in quotes because one may interpret[1,22,23] the 300°K reflectance[7] of magnetite and its transport properties[22,23] as indicating that above T_V small polarons are formed.[12]

As S was determined to be less than 10^{-4} and as the results are in good agreement with previous reflectance measurements, we did not make a correction for S when using Eq. (1) to calculate α from the results shown in Figs. 2(a) and 2(b). These values of α are shown in Fig. 2(c). They are in the range that one would expect[1] for d-band to d-band transitions and are very close to the results[13] obtained with semiconducting V_2O_3.

In view of the many absorption processes that can take place in the spectral range under study,[4] the relatively weak absorption due to the d-band to d-band transitions, and the lack of published data for optical and transport properties we can only analyze the gross features of the data obtained. It is well established from the many conductivity measurements that the conductivity activation *gap* drops from 0.3 to 0.08 eV at T_t. From the present results we know that the optical gap does not change through the transition and thus we conclude that the optical gap is not the conductivity gap above the transition temperature. From the following discussion it appears that there are good reasons to believe that the activation energy just below T_t corresponds to the observed optical gap while the activation energy just above T_t corresponds to the value of E_{VW} just above T_t. This in turn sheds light on the thermoelectric-power and the Hall-effect data as will be discussed below.

We propose that 0.3 eV correspond to transitions between the MW valence band and a "broader" band. In view of the α values obtained, the "broader" band is likely to be the lowest-lying spin-up d-doublet band. The conductivity in this band is more bandlike (and thus we may call it "broader") in contrast to that of the MW bands, and thus this "broader" band contributes most to the conduction for $T < T_t$. That the d-doublet band has a bandlike conduction is not unexpected in view of the effect of degeneracy on conduction in narrow bands.[21] At the transition, E_{VW} collapses from its unknown value below T_t to about 0.08 eV and the main contribution to the conduction is due to the rather narrow MW conduction band. If polarons are formed,[12,22] E_{VW} is smaller than this value. Above T_t, the gap E_{VW} continuously decreases with increasing temperature.

There are four pieces of evidence that support the above interpretation: (1) Lavine[24] found that the thermoelectric power above the transition increases with temperature and this was interpreted[22,23] as due to conduction in a narrow band. This and the fact that Siemons[25] found the same value of thermoelectric power for 77 and 300 K indicate that this power decreases with temperature for $T < T_t$ and bandlike conduction is dominant in this temperature regime. (2) Siemons found that for $T < T_t$ the Hall mobility decreases with temperature, it drops through the transition, and then for $T > T_t$ it increases with temperature in agreement with (1) and with our suggestion. (The low Hall mobility for $T < T_t$ is due to carrier scattering due to optical phonons that might make the measured Hall mobility much smaller than the drift mobility.[6]) (3) In contrast to V_2O_3 and VO_2,[1] the conductivity of Fe_3O_4 increases with increasing temperature above T_t and the sharp collapse of the activation energy at T_t is followed by a continuous shrinkage of this energy as the temperature increases. (4) Our proposed interpretation is very much in accord with the band model of Cullen and Callen[4] and the experimental evidence on which it is based. According to their model, the correlation gap should be *indirect* and since the absorption due to other processes has an α of the order of 10^3 cm^{-1} it should not be seen by the present optical measurements. The possible physical reasons for the collapse of the activation gap and their connection to the Cullen and Callen[4] model will be discussed elsewhere.[11]

The authors are indebted to Dr. S. Freeman for many helpful discussions and to Dr. W. R. Roach for his help in the experiments. Useful comments by Dr. Z. Zinamon and Professor M.

Weger, and the technical help of A. W. Wicklund, C. R. Fuselier, and H. D. Hanson are gratefully acknowledged.

*Work supported in part by the Department of the Navy, Naval Research Laboratory, under Contract No. N00014-71-C-0371.

[1]J. H. de Boer and E. J. W. Verwey, Proc. Phys Soc., London 49, 59 (1937).
[2]E. J. W. Verwey and P. W. Haayman, Physica (Utrecht) 8, 979 (1941).
[3]D. Adler, Solid State Phys. 21, 1 (1968).
[4]D. Adler, Rev. Mod. Phys. 40, 714 (1968).
[5]A. A. Samokhvalov, N. M. Tutikov, and G. P. Skornyakov, Fiz. Tverd. Tela 10, 2760 (1968) [Sov. Phys. Solid State 10, 2172 (1969)].
[6]P. A. Miles, W. B. Westphal, and A. von Hippel, Rev. Mod. Phys. 29, 279 (1957).
[7]R. D. Waldron, Phys. Rev. 99, 1727 (1955).
[8]J. R. Cullen and E. Callen, Phys. Rev. Lett. 26, 236 (1971).
[9]D. Adler and J. Feinleib, Phys. Rev. B 2, 3112 (1970).
[10]N. F. Mott, Advan. Phys. 16, 49 (1967).
[11]G. A. Samara, Phys. Rev. Lett. 21, 795 (1968).
[12]N. F. Mott, Phil. Mag. 20, 1 (1969).
[13]J. B. Sokoloff, Phys. Rev. B 3, 3162 (1971).
[14]I. Balberg and H. Pinch, to be published.
[15]J. Feinleib and W. Paul, Phys. Rev. 155, 841 (1967).
[16]A. S. Barker, Jr., and J. P. Remeika, Solid State Commun. 8, 1521 (1970).
[17]H. W. Verleur, A. S. Barker, Jr., and C. N. Berglund, Phys. Rev. 172, 788 (1968).
[18]L. A. Ladd and W. Paul, Solid State Commun. 7, 425 (1969).
[19]C. A. Domenicali, Phys. Rev. 78, 458 (1950).
[20]J. M. Lavine, Phys. Rev. 114, 482 (1959).
[21]W. F. Brinkman and T. M. Rice, Phys. Rev. B 2, 1324 (1970).
[22]I. G. Austin and C. E. Turner, Phil. Mag. 19, 939 (1969).
[23]W. Haubenreisser, Phys. Status Solidi 1, 619 (1961).
[24]R. A. Bari, D. Adler, and R. V. Lange, Phys. Rev. B 2, 2898 (1970).
[25]J. W. Siemons, IBM J. Res. Develop. 14, 245 (1970).

APPENDIX D

VOLUME 27, NUMBER 20 PHYSICAL REVIEW LETTERS 15 NOVEMBER 1971

Cathodoluminescence of Magnetite*

I. Balberg and J. I. Pankove
RCA Laboratories, Princeton, New Jersey 08540
(Received 1 September 1971)

The cathodoluminescence spectrum of magnetite indicates optical transitions which correspond to energy separations of 2.6 and 3.2 eV. These luminescence data, coupled to the available optical absorption and soft x-ray data, lead to the first proposed semiquantitative band model for this material.

In the study of the electronic structure of the transition-metal oxides, the spectroscopic methods used thus far have been optical transmission and reflectance[1-5] and soft x-ray measurements.[6-8] The lack of large and thin crystals makes optical measurements very difficult[2] and does not permit easy distinction between band-to-band transitions and other absorption processes. X-ray data are not always easy to interpret and no resolution of better than 0.3–0.5 eV has been reported so far. In this Letter we propose a third method: the study of cathodoluminescence. This method has advantages in the above respects and is complementary to optical absorption studies. Further, we shall show how the combined data from all the above-mentioned methods can lead to a quite reliable picture of the band separations in these materials. We report here the first luminescence observation in transition-metal oxides and suggest the first semiquantitative band structure of magnetite (Fe_3O_4).

For the cathodoluminescence study of Fe_3O_4 we have used the natural magnetite single crystals from which slices were cut for our previous optical measurements.[1] The specimens were fastened to the cold finger of a Dewar equipped with a kinescope-type electron gun and a NaCl window transparent over the range of interest. Excitation was provided by an electron beam having a current density of about 1 A/cm^2 at 20 keV. The beam was pulsed for 0.5 μsec every 200 μsec. The infrared region was studied with a Perkin-Elmer 112 spectrometer equipped with a NaCl prism and a thermocouple detector. For the visible luminescence a quartz prism was used and the detector consisted of an RCA 8575 photomultiplier.

The resulting emission spectrum at two temperatures is shown in Fig. 1. Clearly, there is an emission peak at photon energy $h\nu = 2.6$ eV and a shoulder which is attributable to another peak at about 3.2 eV. The difference in intensities at the two temperatures is probably due to the usual increase in nonradiative processes with increasing temperature. The nonradiative recombination may be enhanced in the present case as the sample passes through the "semiconductor-to-metal" transition when heated from 77 to 300°K. The possible smearing of the 3.2-eV shoulder at 300°K will be discussed below. No other luminescence has been observed in the spectral range $0.1 \leq h\nu \leq 4$ eV. We shall first

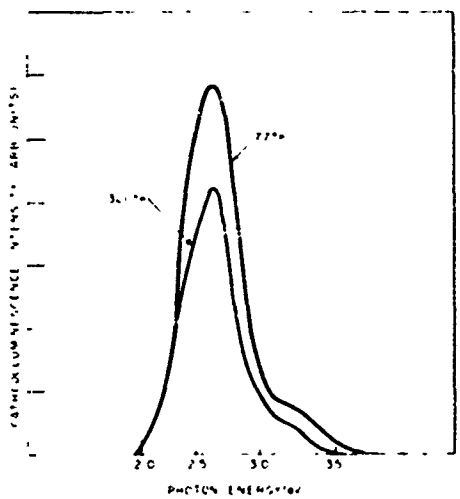

FIG. D-1. Cathodoluminescence spectra of Fe_3O_4.

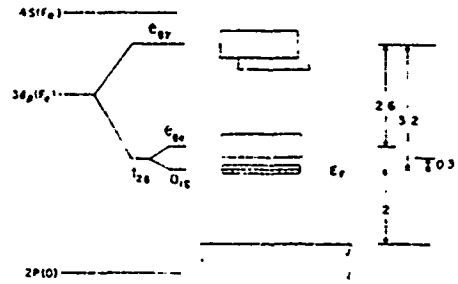

FIG. D-2. Atomic level scheme of an octahedral site in Fe_3O_4, and the proposed energy separations between the corresponding bands in the "metallic" phase.

interpret the results for the "metallic" phase of Fe_3O_4, since only room-temperature soft x-ray studies were reported for this material,[8] and later on we shall discuss the results for the "semiconducting" phase of this material.

The transitions associated with the observed cathodoluminescence are from some high-lying band to some lower empty band to which the transition has a considerable probability. Thus, in trying to interpret the data we should first look for the available bands and for the expected strong transition probabilities. As is widely accepted, when one examines the $3d^n$ transition-metal oxides, the broadening of the atomic d levels into bands decreases with increasing z, and correspondingly, the crystal-field approach becomes more and more appropriate.[9] For $z \sim 5$, the $3d$ levels are split by the difference in their respective exchange potentials Δ_{ex} (which in the case of MnO is about 6 eV). One can thus talk about the five spin-down (or $3d_\beta$) electrons and about the rest of the electrons in the $3d$ shell as spin-up (or $3d_\alpha$) electrons.[9] For NiO and α-Fe_2O_3, which are expected[10] to have a band structure similar to FeO or Fe_3O_4 and for which the relevant information is available, it has been established[10-12] that the lowest bands that emerge from the $3d_\beta$ level are, respectively, about 1.5 and 2 eV higher than the oxygen $2p$ band. Thus it can be safely assumed that in FeO or Fe_3O_4 the $3d_\beta$ levels lie a few electron volts below the top of the oxygen $2p$ band, and thus are irrelevant to our cathodoluminescence study. Since the oxygen $2p$ $|2p(O)|$ band is filled we should next consider the $3d_\beta$(Fe) levels from which the lowest lying unoccupied bands are formed in the solid.[13] In Fe_3O_4 two types of $3d_\beta$(Fe) levels should be considered: those of the tetrahedral sites that are split by the crystal field to a high-lying t_2 level and a low-lying e level, and those of the octahedral sites that are split to a high-lying e_g level (hereafter referred to as e_{gT}) and a low-lying t_{2g} level.[9,10] The β of the tetrahedral sites corresponds however to a spin opposite to that assigned to the β of the octahedral sites. The t_{2g} octahedral level is further split to a higher lying e_{fg} level and a lower lying a_{1g} level. This results from the trigonal distortion of the crystal field, which, as in FeO, corresponds to a trigonal angle[9,14] that is less than 60°. The energy separation between the last two levels is expected to be[9,10,14] much smaller than the e_{gT}-t_{2g} separation. Since all these levels broaden into bands, we shall from now on refer to them as bands and call them by the name of the levels from which they emerge. The octahedral crystal-field splitting is illustrated in the left-hand side of Fig. 2.

It is well established that the electrons which are in the highest occupied band "belong" to the octahedral sites.[13,15,16] Since the number of $3d_\beta$ electrons is half the number of the octahedral sites, we expect this band to be half filled.[13] This seems to be the case at least above 300°K and thus we can assume that the Fermi energy E_F lies in the middle of this band.[1,13]

It follows from the above that the lowest accessible band for the luminescence transitions

is this half-filled a_{1g} band. The next higher band, $e_{g\gamma}$, being empty, can also serve as a terminating band for luminescent transitions from a higher lying band. Absorbing transitions from the half-filled a_{1g} band to higher bands should yield a structure in the absorption data. The absorption data, which are available for thin films only[17] (it was found[1,18] to be the same at 77 and at 300 °K), show an absorption edge beginning at 2 eV and extending to above 6 eV. There is a pronounced bump on this absorption edge extending from 2.3 to 3.5 eV and having a maximum at 3.2 eV. Other information comes from soft x-ray data.[6] There, one finds that the energy separation between the x-ray absorption and emission peaks is 2.7 ± 0.5 eV and no other structure is found between these peaks, in accord with our data. Further, the x-ray data[6] show that about 2 eV below the x-ray emission peak there is a shoulder below which no other structure can be detected. In view of other soft x-ray data in transition-metal oxides[6,7] it seems very likely that this shoulder is associated with a transition from the oxygen $2p$ band to the iron $2p$ level, and thus E_F is expected to lie about 2 eV above the top of the $2p$(O) band. This is also consistent with the values given above for the corresponding energy separation in NiO and α-Fe_2O_3. It is conceivable that the 2-eV onset of the absorption edge is determined by the separation between E_f and the $2p$(O) band.

From all the above data it appears that the observed luminescence is due to transitions from a band that lies about 3.2 eV above E_F to the $e_{g\gamma}$ band and to the half-filled a_{1g} band. This suggestion is further supported by the relative intensities of the 2.6- and 3.2-eV peaks, since the number of empty states in the $e_{g\gamma}$ band is four times larger than their number in the half-filled a_{1g} band. The results then indicate that the energy separation between E_f and the center of the $e_{g\gamma}$ band is about 0.6 eV. This is very much in accord with our recent optical measurements[1] that indicate a 0.3-eV energy separation between E_f and the bottom of the $e_{g\gamma}$ band. From both results we can even estimate the width of the $e_{g\gamma}$ band to be about 0.6 eV. This is also consistent with our suggestion[1] that the $e_{g\gamma}$ band gives rise to band-like conduction. From the absorption data it appears that the band the center of which lies about 3.2 eV above E_F has a width of about 0.7 eV. As the optical absorption edge is reminiscent of that identified[11] in NiO as due to the $3d^8 - 4s$ transitions in its spectral shape, absolute value, and energy range, it can be tentatively concluded that it is associated with the 4s(Fe) band. Consistent with the energy separation between the d_β bands[11] in NiO and also with the above crystal field approach, it further seems natural to believe that the 0.7-eV-wide band is the $e_{g\gamma}$ band (see below). The start of the optical absorption edge at about 2 eV, and the poor resolution of the x-ray data, only enable us to identify the edge of the 4s(Fe) band as lying 2.5 ± 0.5 eV above E_f. Thus the amount of overlap of the 4s(Fe) and the $e_{g\gamma}$ band is known only to within this accuracy of ± 0.5 eV. On the basis of the above discussion, we show in Fig. 2 the energy separations between the bands that emerge from the $3d_\beta$ level of an octahedral site in Fe_3O_4.

While the locations of the luminescence and soft x-ray peaks are in accord with a "localized" approach based on single-site transitions, the band-theory approach is more helpful in explaining transitions which should be forbidden by the dipole selection rules, as well as the relative intensities of the observed transitions. The applicability in part of each of these approaches[12] is not surprising in the present case, since Fe_3O_4 is believed to exhibit a Mott-Wigner transition.[1,12,18,19] First, from band theory all the bands considered above are expected to have some s character that originates from the 2s(O)[20-22] and the 3s(O)[23] orbitals. While the influence of the 2s(O) orbitals on the band structure was calculated,[20-22] the influence of the 3s(O) was not.[20] In view of the estimated[23] separation of the $2p$(O)-3s(O) bands, and the calculated[21,22] separation of the 2s(O)-$2p$(O) bands, it appears that the contribution of the 3s(O) orbitals can be even larger than that of the 2s(O) orbitals. For the present discussion, however, it is enough to note that an s character is found in all the bands shown in Fig. 2. Also from band theory the $e_{g\gamma}$ and the a_{1g} bands are expected[8,20-22] to have some $2p$(O) character and this d-p mixing should be quite strong in magnetite in view of the high Néel temperature (850°K). Finally, the $e_{g\gamma}$ band is expected[8,20-22] to be hybridized with the 4s(Fe) band. All this explains the observation of the $2p$(O) $-$ $2p$(Fe) soft x-ray transition,[23] the observation of optical absorption associated with interband transition in the t_{2g} subshell,[1-5] and the much higher transition probabilities for the $e_{g\gamma} - e_{g\epsilon}$ and the $e_{g\gamma} - a_{1g}$ transitions compared with that of the $e_{g\epsilon} - a_{1g}$ transition (no luminescence has been detected for the latter transition and the optical absorption coefficient was found to be quite small[1]). This supports our interpretation

that the strong 2.6-eV cathodoluminescence peak is due to transitions from the maximum in the density of states of the $4s(\mathrm{Fe})+e_{g}$ band to the maximum in the density of states of the e_{g} band, and similarly that the 3.2-eV luminescence corresponds to the $4s(\mathrm{Fe})+e_{g}-a_{1g}$ transitions.

In all the data available, there is no evidence for other bands between the e_{g} and the $4s(\mathrm{Fe})+e_{g}$ bands. As the crystal-field splitting of the tetrahedral sites is expected to be smaller than that of the octahedral sites (theoretically by a factor of $\frac{4}{9}$), the experimental observations can be interpreted in two ways: (a) If we believe that the inverse spinel stabilization energy is just the disordering energy of the octahedral sites[24] and that some short-range order in these sites prevails to very high temperatures, we should conclude that the octahedral-site to tetrahedral-site transition has a very low transition probability. (b) If the inverse spinel stabilization energy is larger than the disordering energy,[24] it may be that the stabilization energy is beyond the spectral range under study.

Below the "semiconductor-to-metal" transition temperature, the a_{1g} band splits because of interatomic correlation[13,19] but the amount of this splitting is unknown. (In view of previous[1] and present data this splitting energy E_{s} is probably between 0.3 and 0.9 eV.) At 77°K we still have about 10^{18} vacancies in the "Mott-Wigner valence band"[1] and in the gap between this band and the e_{g} band[1] (since this is the number of carriers at this temperature). This number may be even larger because of the excitation by the electron beam. Thus the radiative transition from $4s(\mathrm{Fe})+e_{g}$ to the vicinity of the "Mott-Wigner valence band"[1] is still quite strong and still close to 3.2 eV.

In conclusion, we have presented the cathodoluminescence spectrum of Fe_3O_4 by which we were guided in interpreting the existing optical and soft x-ray data of this material. It seems now that one can explain the data available for Fe_3O_4 by the expected band structure of the transition-metal monoxides, and that the so far unexplored FeO has a band structure quite similar to that of Fe_3O_4.

The authors are indebted to J. E. Berkeyheiser, Jr., for his skillful help in the measurements.

---

*Work supported in part by the Department of the Navy, Naval Research Laboratory under Contract No. N00014-71-C-0371.

[1]I. Balberg and J. I. Pankove, Phys. Rev. Lett. 27, 596 (1971).
[2]L. A. Ladd and W. Paul, Solid State Commun. 7, 425 (1969).
[3]H. W. Verleur, A. S. Barker, Jr., and C. N. Berglund, Phys. Rev. 172, 788 (1968).
[4]J. Feinleib and W. Paul, Phys. Rev. 155, 841 (1967).
[5]A. S. Barker, Jr., and J. P. Remeika, Solid State Commun. 8, 1521 (1970).
[6]D. W. Fischer and W. L. Baun, J. Appl. Phys. 39, 4757 (1968).
[7]D. W. Fischer, J. Appl. Phys. 40, 4151 (1969).
[8]C. Bonnelle, Ann. Phys. (Paris) 1, 439 (1966).
[9]T. M. Wilson, Int. J. Quant. Chem., Symp. 1970, 757.
[10]F. J. Morin, in *Semiconductors*, edited by N. B. Hannay (Cambridge U. Press, Cambridge, England, 1959), p. 600.
[11]D. Adler and J. Feinleib, Phys. Rev. B 2, 3112 (1970).
[12]D. Adler, in *Solid State Physics*, edited by H. Ehrenreich, F. Seitz, and D. Turnbull (Academic, New York, 1968), Vol. 21, p. 1.
[13]J. R. Cullen and E. Callen, Phys. Rev. Lett. 26, 236 (1971).
[14]K. Yosida and M. Tachiki, Progr. Theor. Phys. 17, 331 (1957).
[15]R. S. Hargrove and W. Kündig, Solid State Commun. 8, 303 (1970).
[16]W. C. Hamilton, Phys. Rev. 110, 1050 (1958).
[17]P. A. Miles, W. B. Westphal, and A. von Hippel, Rev. Mod. Phys. 29, 279 (1957).
[18]I. Balberg and H. Pinch, to be published.
[19]N. F. Mott, Phil. Mag. 20, 1 (1969).
[20]T. E. Norwood and J. L. Fry, Phys. Rev. B 2, 472 (1970).
[21]V. Ern and A. C. Switendick, Phys. Rev. 137, 1927 (1965).
[22]A. C. Switendick, Massachusetts Institute of Technology Solid State and Molecular Theory Group Quarterly Progress Report No. 49, 1963 (unpublished), p. 41.
[23]D. Adler, J. Chem. Phys. 52, 4908 (1970).
[24]F. DeBoer, J. H. VanSanten, and E. J. Verwey, J. Chem. Phys. 18, 1032 (1950).